

BLEJSKE DELAVNICE IZ FIZIKE

BLED WORKSHOPS IN PHYSICS

LETNIK 17, ŠT. 1

VOL. 17, NO. 1

ISSN 1580-4992

Proceedings of the Mini-Workshop
Quarks, Hadrons, Matter

Bled, Slovenia, July 3 – 10, 2016

Edited by

Bojan Golli

Mitja Rosina

Simon Širca

University of Ljubljana and Jožef Stefan Institute

DMFA – ZALOŽNIŠTVO
LJUBLJANA, NOVEMBER 2016

The Mini-Workshop *Quarks, Hadrons, Matter*

was organized by

*Society of Mathematicians, Physicists and Astronomers of Slovenia
Department of Physics, Faculty of Mathematics and Physics, University of Ljubljana*

and sponsored by

*Department of Physics, Faculty of Mathematics and Physics, University of Ljubljana
Jožef Stefan Institute, Ljubljana
Society of Mathematicians, Physicists and Astronomers of Slovenia*

Organizing Committee

Mitja Rosina, Bojan Golli, Simon Širca

List of participants

*Marko Bračko, Ljubljana, marko.bracko@ijs.si
Wojtek Broniowski, Krakow, b4bronio@cyf-kr.edu.pl
Michael Buballa, Darmstadt, buballa@theorie.i.kp.physik.tu-darmstadt.de
Thomas Cohen, Maryland, cohen@physics.umd.edu
Bojan Golli, Ljubljana, bojan.golli@ijs.si
Ju-Hyun Jung, Graz, ju.jung@uni-graz.at
Bogdan Povh, Heidelberg, b.povh@mpi-hd.mpg.de
Christian Rohrhofer, Graz, christian.rohrhofer@uni-graz.at
Mitja Rosina, Ljubljana, mitja.rosina@ijs.si
Ica Stancu, Liege, fstancu@ulg.ac.be
Simon Širca, Ljubljana, simon.sirca@fmf.uni-lj.si
Sachiko Takeuchi, Tokio, s.takeuchi@jcsu.ac.jp
Herbert Weigel, Stellenbosch, weigel@sun.ac.za*

Electronic edition

<http://www-f1.ijs.si/BledPub/>

Contents

Preface	V
Predgovor	VII
Limits on hadron spectrum from bulk medium properties	
<i>Wojciech Broniowski</i>	1
What can we learn from NJL-type models about dense matter?	
<i>Michael Buballa</i>	6
The Sign Problem in QCD	
<i>Thomas D. Cohen</i>	12
The microscopic structure of πNN, $\pi N\Delta$ and $\pi\Delta\Delta$ vertices in a hybrid constituent quark model	
<i>Ju-Hyun Jung and Wolfgang Schweiger</i>	13
The nucleon spin in deep inelastic scattering	
<i>Bogdan Povh</i>	19
Angular momentum content of the $\rho(1450)$ from chiral lattice fermions	
<i>C. Rohrhofer, M. Pak, L. Ya. Glozman</i>	20
Excited hyperons of the $N = 2$ band in the $1/N_c$ expansion	
<i>Fl. Stancu</i>	25
$c\bar{c}$-pentaquarks by a quark model	
<i>Sachiko Takeuchi</i>	32
Soliton model analysis of SU(3) symmetry breaking for baryons with a heavy quark	
<i>H. Weigel, J. P. Blanckenberg</i>	33
Selected Recent Results from Belle on Hadron Spectroscopy	
<i>M. Bračko</i>	38

Puzzles in eta photoproduction: the 1685 MeV narrow peak	
<i>B. Golli and S. Širca</i>	44
The equation of state in the quasispin Nambu–Jona-Lasinio model	
<i>Mitja Rosina</i>	50
The perennial Roper puzzle	
<i>S. Širca</i>	55
Povzetki v slovenščini	59

Preface

Our traditional Mini-Workshop at Bled carried some resemblance to a “forma viva”, a colony of sculptors modelling their statues with their unique idea and individual method. The friendly interactions helped us to polish the models and to understand their implications. The progress we have made is preserved in these Proceedings in order to stimulate further interactions in the years to come.

This year, one of the questions was what can we learn from the Nambu–Jona-Lasinio (NJL) model and other models about the QCD and hadronic phases and about the *dense and/or hot quark matter*, also in the context of compact stars. While in general the results should not be trusted quantitatively, the NJL model is a powerful theoretical tool for obtaining new insights and ideas. An interesting aspect of Lattice QCD was also presented: the bulk thermal properties of the hadron gas preclude a very fast rising of the number of resonances, as assumed by the Hagedorn hypothesis, unless a substantial repulsion between hadronic resonances is present.

Another focus was the *light hadron spectroscopy and nucleon structure*. The classification of excited baryons into SU(3) singlets, octets and decuplets, as supported by the $1/N_c$ expansion, has been extended to strange baryons. Puzzles in η photoproduction were related to low-lying resonances and the opening of a nearby threshold rather than to an exotic resonance. The elusive Roper resonance has been approached with models involving meson-baryon or meson-quark dressing, with Lattice QCD and, experimentally, through pion electroproduction. The quark spin content of the nucleon and its relation to the pion cloud is still unclear. The pion cloud is also responsible for the pion-baryon-baryon vertices. The chiral and angular momentum content confirms the $\rho(770)$ to be a 3S_1 state, in accordance with the quark model, while the $\rho(1450)$ is a 3D_1 and not a radial excitation of the $\rho(770)$.

The third emphasis was on *new resonances in the charm sector*. The meson and baryon resonances discovered at the Belle detector at KEKB are still being analyzed in order to determine their quantum numbers and their double- $q\bar{q}$ or “molecular” dimeson structure. For the spectrum of baryons with one heavy and two light quarks, the collective-coordinate Hamiltonian in the chiral soliton model was proposed. After the failure of the light pentaquark, there is a revived interest in heavy pentaquarks. A good candidate is the $P_c(4380)$ resonance, since the color-magnetic interaction which causes a repulsion between the nucleons can result in an attraction in the color-octet configuration.

We would like to thank again all participants for coming and for making the Mini-Workshop so friendly, lively and fruitful. We shall be happy to see you again at Bled, either next year or thereafter.

Predgovor

Naša tradicionalna blejska delavnica spominja na “formo vivo”, kiparsko kolonijo, kjer vsak modelira svojo mojstrovino s svojo značilno idejo in metodo. Prijateljsko povezovanje nam je pomagalo izbrusiti modele in razumeti njihove implikacije. Doseženi napredek je zabeležen v tem Zborniku — v spodbudo za nadaljnje sodelovanje v prihodnjih letih.

Letos je bilo eno od odprtih vprašanj, kaj se iz Nambu–Jona-Lasiniovega (NJL) in drugih modelov lahko naučimo o kromodinamskem in hadronskem faznem diagramu in o lastnostih *goste in/ali vroče kvarkovske snovi*, zlasti v povezavi s kompaktnimi zvezdami. Čeprav rezultatom v splošnem ne moremo zaupati kvantitativno, je model NJL močno teoretično orodje za nove vpogleda in zamisli. Predstavljen je bil tudi zanimiv vidik kromodinamike na mreži: termodinamske lastnosti hadronskega plina izključujejo hitro naraščanje števila resonanc (kot jih predvideva Hagedornova hipoteza), razen če obstaja znaten odboj med hadronskimi resonancami.

Drugo žarišče razprav sta bili *spektroskopija lahkih hadronov in zgradba nukleona*. Klasifikacija vzbujenih stanj barionov v singlete, oktete in deplete simetrije SU(3), kot jo podpira razvoj po recipročnem številu barv, je bila razširjena na čudne barione. Uganke pri fotoprodukciji mezona η so navezali na nizko ležeče resonance in odprte bližnje kanale, ne kažejo pa na eksotične resonance. Izmužljive Roperjeve resonance so se lotili z modeli, ki vključujejo oblačenje barionov in kvarkov z mezoni, pa tudi s kromodinamiko na mreži in eksperimentalno z elektroprodukcijo pionov. Delež kvarkovskega spina v nukleonu in njegova povezava s pionskim oblakom je še nejasna. Pionski oblak je tudi odgovoren za vozlišča med pioni in barioni. Delež kiralnosti in vrtilne količine potrjuje, da je mezon $\rho(770)$ v stanju 3S_1 v skladu s kvarkovskim modelom, medtem ko je mezon $\rho(1450)$ v stanju 3D_1 in ni radialno vzbujeno stanje mezona $\rho(770)$.

Tretje težišče predstavitev so bile *nove resonance v čarobnem sektorju*. Mezonske in barionske resonance, odkrite z detektorjem Belle pri pospeševalniku KEKB, še vedno analizirajo, da bi določili njihova kvantna števila ter njihovo zgradbo kot dveh parov $q\bar{q}$ ali dvomezonske molekule. Za spekter barionov iz enega težkega in dveh lahkih kvarkov je bila predlagana metoda kolektivnih koordinat v kiralnem solitonskem modelu. Po neuspehu lahkega pentakvarka je naraslo zanimanje za težke pentakvarke. Dober kandidat je resonanca $P_c(4380)$, kajti kromomagnetna interakcija, ki povzroči odboj med nukleonoma, lahko vodi do privlaka v barvno oktetni konfiguraciji sestavin pentakvarka.

Radi bi se ponovno zahvalili vsem udeležencem, da ste prišli in naredili našo mini-delavnico tako prijazno, živahno in plodno. Veseli bomo, če vas bomo na Bledu spet videli prihodnje leto ali kmalu zatem.

Workshops organized at Bled

- ▷ *What Comes beyond the Standard Model*
(June 29–July 9, 1998), Vol. **0** (1999) No. 1
(July 22–31, 1999)
(July 17–31, 2000)
(July 16–28, 2001), Vol. **2** (2001) No. 2
(July 14–25, 2002), Vol. **3** (2002) No. 4
(July 18–28, 2003) Vol. **4** (2003) Nos. 2-3
(July 19–31, 2004), Vol. **5** (2004) No. 2
(July 19–29, 2005) , Vol. **6** (2005) No. 2
(September 16–26, 2006), Vol. **7** (2006) No. 2
(July 17–27, 2007), Vol. **8** (2007) No. 2
(July 15–25, 2008), Vol. **9** (2008) No. 2
(July 14–24, 2009), Vol. **10** (2009) No. 2
(July 12–22, 2010), Vol. **11** (2010) No. 2
(July 11–21, 2011), Vol. **12** (2011) No. 2
(July 9–19, 2012), Vol. **13** (2012) No. 2
(July 14–21, 2013), Vol. **14** (2013) No. 2
(July 20–28, 2014), Vol. **15** (2014) No. 2
(July 11–20, 2015), Vol. **16** (2015) No. 2
(July 11–19, 2016), Vol. **17** (2016) No. 2
- ▷ *Hadrons as Solitons* (July 6–17, 1999)
- ▷ *Few-Quark Problems* (July 8–15, 2000), Vol. **1** (2000) No. 1
- ▷ *Statistical Mechanics of Complex Systems* (August 27–September 2, 2000)
- ▷ *Selected Few-Body Problems in Hadronic and Atomic Physics* (July 7–14, 2001),
Vol. **2** (2001) No. 1
- ▷ *Studies of Elementary Steps of Radical Reactions in Atmospheric Chemistry*
(August 25–28, 2001)
- ▷ *Quarks and Hadrons* (July 6–13, 2002), Vol. **3** (2002) No. 3
- ▷ *Effective Quark-Quark Interaction* (July 7–14, 2003), Vol. **4** (2003) No. 1
- ▷ *Quark Dynamics* (July 12–19, 2004), Vol. **5** (2004) No. 1
- ▷ *Exciting Hadrons* (July 11–18, 2005), Vol. **6** (2005) No. 1
- ▷ *Progress in Quark Models* (July 10–17, 2006), Vol. **7** (2006) No. 1
- ▷ *Hadron Structure and Lattice QCD* (July 9–16, 2007), Vol. **8** (2007) No. 1
- ▷ *Few-Quark States and the Continuum* (September 15–22, 2008),
Vol. **9** (2008) No. 1
- ▷ *Problems in Multi-Quark States* (June 29–July 6, 2009), Vol. **10** (2009) No. 1
- ▷ *Dressing Hadrons* (July 4–11, 2010), Vol. **11** (2010) No. 1
- ▷ *Understanding hadronic spectra* (July 3–10, 2011), Vol. **12** (2011) No. 1
- ▷ *Hadronic Resonances* (July 1–8, 2012), Vol. **13** (2012) No. 1
- ▷ *Looking into Hadrons* (July 7–14, 2013), Vol. **14** (2013) No. 1
- ▷ *Quark Masses and Hadron Spectra* (July 6–13, 2014), Vol. **15** (2014) No. 1
- ▷ *Exploring Hadron Resonances* (July 5–11, 2015), Vol. **16** (2015) No. 1
- ▷ *Quarks, Hadrons, Matter* (July 3–10, 2016), Vol. **17** (2016) No. 1





Limits on hadron spectrum from bulk medium properties^{*}

Wojciech Broniowski^{a,b}

^a Institute of Physics, Jan Kochanowski University 25-406 Kielce, Poland

^b The H. Niewodniczański Institute of Nuclear Physics Polish Academy of Sciences, 31-342 Cracow, Poland

Abstract. We bring up the fact that the bulk thermal properties of the hadron gas, as measured on the lattice, preclude a very fast rising of the number of resonance states in the QCD spectrum, as assumed by the Hagedorn hypothesis, unless a substantial repulsion between hadronic resonances is present. If the Hagedorn growth continued above masses ~ 1.8 GeV, then the thermodynamic functions would noticeably depart from the measured lattice values at temperatures above 140 MeV, just below the transition temperature to quark-gluon plasma.

In this talk we point out the sensitivity of thermal bulk medium properties (energy density, entropy, sound velocity...) to the spectrum of the hadron resonance gas. In particular, we explore the effects of the high-lying part of the spectrum, above ~ 1.8 GeV, where it is poorly known, on the thermal properties still below the cross-over transition to the quark-gluon plasma phase. Such investigations were carried out in the past by various authors, see [1–5] and references therein, where the reader may find more details and results.

The presently established QCD spectrum reaches about 2 GeV, and it is a priori not clear what happens above. Does the growth continue, or is saturated? As is evident from Fig. 1, the Hagedorn hypothesis [7] works very well up to about 1.8 GeV [8]. In the following, we explore two models: 1) hadron resonance gas with the Breit-Wigner width, HRG(Γ), which takes into account all states listed in the Particle Data Group tables [6] with mass below 1.8 GeV, and 2) this model amended with the states above 1.8 GeV, modeled with the Hagedorn formula fitted to the spectrum at lower masses (see Fig. 1). In short, model 1) includes the up-to-now established resonances, and model 2) extends them according to the Hagedorn hypothesis.

First, we recall the fact that the inclusion of widths of resonances [11], as listed in the Particle Data Group tables, affects the results noticeably and in fact improves them. This is shown in Fig. 2, where the hadron resonance gas calculation for the QCD trace anomaly, $\epsilon - 3p$ divided by T^4 . Here ϵ stands for the energy density, p for the pressure, and T for the temperature. In the calculation,

^{*} Supported by the Polish National Science Centre grants DEC-2015/19/B/ST2/00937 and DEC-2012/06/A/ST2/00390.

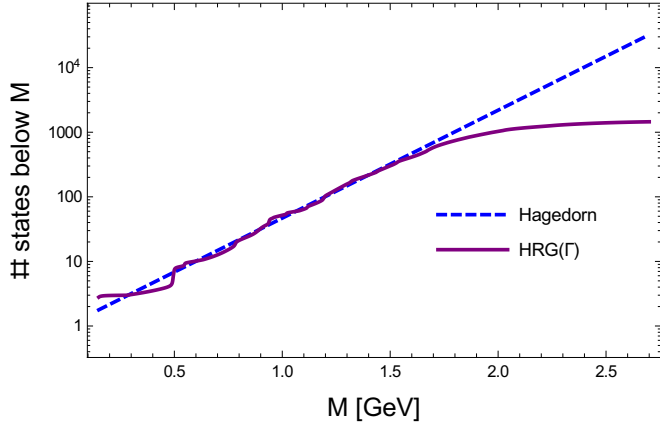


Fig. 1. Solid line, labeled HRG(Γ): Number of QCD states (mesons, baryons, and antibaryons combined) with mass below M . All stable particles and resonances from the Particle Data Group tables [6] are included and their Breit-Wigner width is taken into account. Dashed line: the fit with the Hagedorn formula for the density of states, $\rho(m) = \Lambda \exp(m/T_H)$, with $T_H = 260$ MeV.

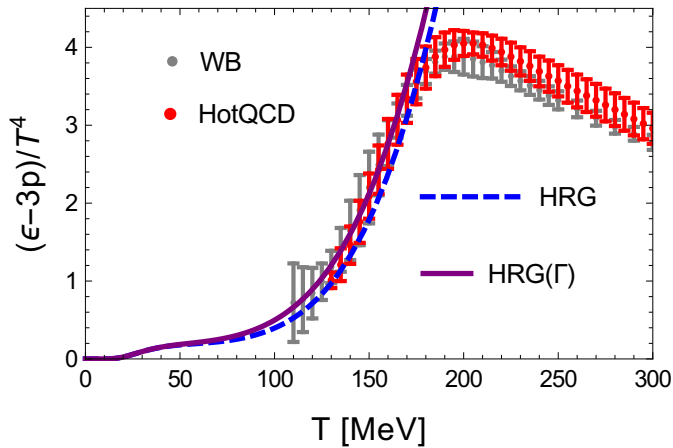


Fig. 2. The QCD trace anomaly (divided by T^4) plotted as a function of temperature T . The inclusion of width of resonances to the hadron resonance gas improves the agreement with the lattice data from the Wuppertal-Budapest (WB) [9] and Hot QCD [10] collaborations.

the hadrons are treated as components of an ideal gas of fermions and bosons. We note that the overall agreement with of the hadron resonance gas model HRG(Γ) with the lattice measurement is remarkable.

The virial expansion of Kamerlingh Onnes yields $p/T = \rho + B_2(T)\rho^2 + B_3(T)\rho^3 + \dots$. Correspondingly, for the partition function of a thermodynamic system including the $1 \rightarrow 1$, $2 \rightarrow 2$, etc., processes one has

$$\ln Z = \ln Z^{(1)} + \ln Z^{(2)} + \dots \quad (1)$$

The non-interacting term

$$\ln Z^{(1)} = \sum_{\mathbf{k}} \ln Z_{\mathbf{k}}^{\text{stable}} = \sum_{\mathbf{k}} f_{\mathbf{k}} V \int \frac{d^3 p}{(2\pi)^3} \ln \left[1 \pm e^{-E_{\mathbf{p}}/T} \right]^{\pm 1} \quad (2)$$

includes the sum over all stable particles, whereas the second-order virial term involves the sum over pairs of stable particles denoted as K ,

$$\ln Z^{(2)} = \sum_{\mathbf{K}} f_{\mathbf{K}} V \int_0^{\infty} \frac{d\delta_{\mathbf{K}}(M)}{\pi dM} dM \int \frac{d^3 P}{(2\pi)^3} \ln \left[1 \pm e^{-E_{\mathbf{P}}/T} \right]^{\pm 1}, \quad (3)$$

where $\delta_{\mathbf{K}}(M)$ stands for the phase shift in the channel K . For narrow resonances the correction to the density of two-body states $d\delta_{\mathbf{K}}(M)/(\pi dM)$ [12] can be accurately approximated with the Breit-Wigner form, which is a basis of the hadron resonance gas model.

In Fig. 3 we show the result of extending the Hagedorn hypothesis above the present experimental limit on the QCD spectrum. We note that the inclusion of extra (non-interacting) states above $M = 1.8$ GeV has a quite dramatic effect on the trace anomaly $\theta_{\mu}^{\mu} = \epsilon - 3p$, placing it way above the lattice data at $T > 140$ MeV (the model calculation is credible below $T \simeq 170$ MeV, where a cross-over to the quark-gluon plasma occurs). A similar conclusion is drawn for other thermodynamic quantities, such as the entropy (cf. Fig. 4) or the sound velocity (cf. Fig. 5).

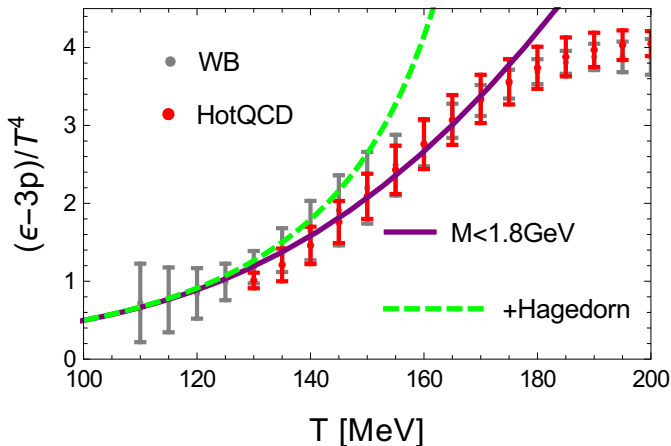


Fig. 3. Same as in Fig. 2 but with the lines denoting the hadron resonance gas model, $\text{HRG}(\Gamma)$, up to $M = 1.8$ GeV, and this model amended with the Hagedorn spectrum above $M = 1.8$ GeV.

Therefore, if the hadron resonances were non-interacting, there would be no room for extra states above 1.8 GeV in the QCD spectrum. This conclusion may be affected by repulsion between the states (e.g., the excluded volume corrections), which decreases the contribution to the partition function. The issue is

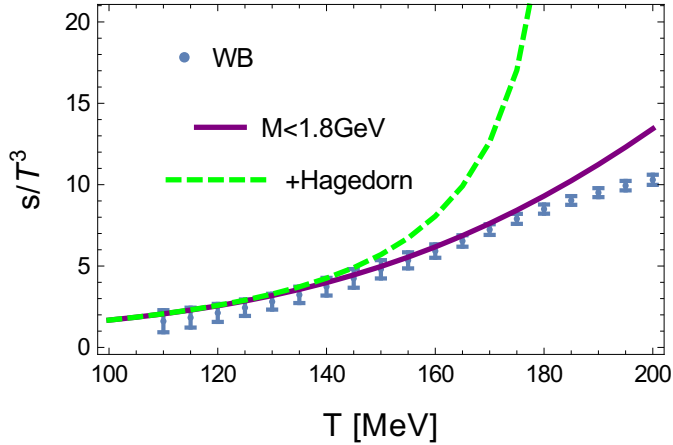


Fig. 4. Same as in Fig. 3 but for the entropy density divided by T^3 .

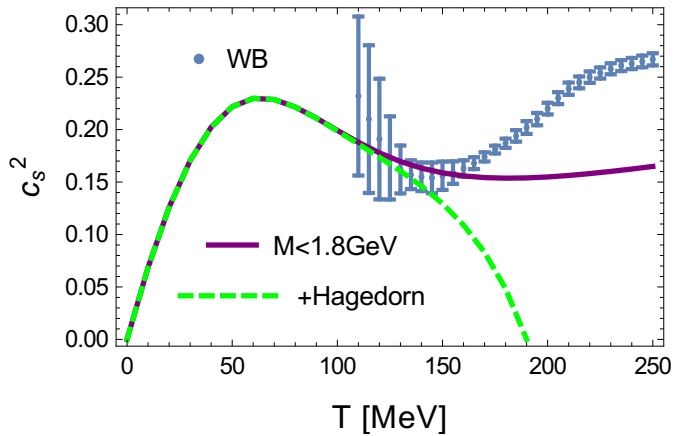


Fig. 5. Same as in Fig. 3 but for the square of the sound velocity.

discussed quantitatively in [3, 4], where a reduction of contributions to the thermodynamic quantities is assessed. The excluded volume reduces the contribution of resonances, and this makes them possible to appear in the spectrum in an “innocuous” way. The effect is explicit in Eq. (3), as repulsion leads to a decrease of the phase shift with M , or a negative correction to the density of states $d\delta_\kappa(M)/(\pi dM)$.

An important example of such an explicit cancellation occurs in the case of the σ meson, whose contribution to one-body observables is canceled by the isospin-2 channel [12]. The case of the trace anomaly is shown in Fig. 6. Note that the phase shift taken into account in this analysis automatically includes the short-distance repulsion in specific channel, hence there is no need to model it separately. The cancellation experienced by the σ state may occur also for other states with higher mass.

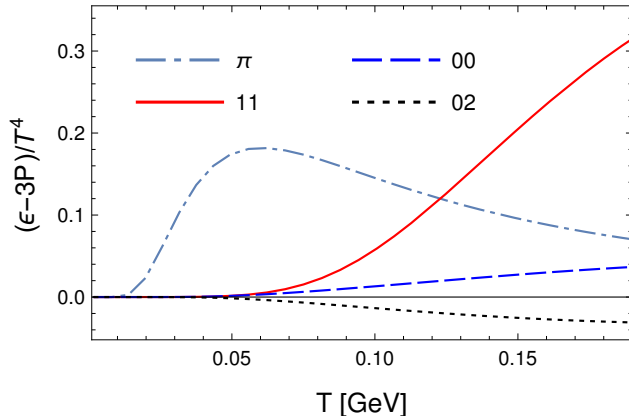


Fig. 6. Contributions to the trace anomaly from the pions, ρ mesons, σ meson, and the isospin-2 component of the pion-pion interaction. We note an almost perfect cancellation of the σ and isospin-2 channels.

In conclusion, the thermodynamic quantities offered by the modern lattice QCD calculations allow to place limits on the high-lying spectrum on the QCD resonances, but the interactions between the states, such as the short-range repulsion, must be properly taken into account, as the two effects: increasing the number of states and introducing repulsion works in the opposite way.

References

1. F. Karsch, K. Redlich, and A. Tawfik, *Eur. Phys. J.* **C29**, 549 (2003), arXiv:hep-ph/0303108 [hep-ph].
2. P. Huovinen and P. Petreczky, *Nucl. Phys.* **A837**, 26 (2010), arXiv:0912.2541 [hep-ph].
3. A. Andronic, P. Braun-Munzinger, J. Stachel, and M. Winn, *Phys. Lett.* **B718**, 80 (2012), arXiv:1201.0693 [nucl-th].
4. E. Ruiz Arriola, L. L. Salcedo, and E. Megias, *54th Cracow School of Theoretical Physics: QCD meets experiment: Zakopane, Poland, June 12-20, 2014*, *Acta Phys. Polon.* **B45**, 2407 (2014), arXiv:1410.3869 [hep-ph].
5. P. M. Lo, M. Marzecenko, K. Redlich, and C. Sasaki, *Phys. Rev.* **C92**, 055206 (2015), arXiv:1507.06398 [nucl-th].
6. K. A. Olive, *Chin. Phys.* **C40**, 100001 (2016).
7. R. Hagedorn, *Nuovo Cim. Suppl.* **3**, 147 (1965).
8. W. Broniowski, W. Florkowski, and L. Ya. Glozman, *Phys. Rev.* **D70**, 117503 (2004), arXiv:hep-ph/0407290 [hep-ph].
9. S. Borsanyi, Z. Fodor, C. Hoelbling, S. D. Katz, S. Krieg, and K. K. Szabo, *Phys. Lett.* **B730**, 99 (2014), arXiv:1309.5258 [hep-lat].
10. A. Bazavov *et al.* (HotQCD), *Phys. Rev.* **D90**, 094503 (2014), arXiv:1407.6387 [hep-lat].
11. E. Ruiz Arriola, W. Broniowski, and P. Masjuan, *Proceedings, Conference on Modern approaches to nonperturbative gauge theories and their applications (Light Cone 2012): Cracow, Poland, July 8-13, 2012*, *Acta Phys. Polon. Supp.* **6**, 95 (2013), arXiv:1210.7153 [hep-ph].
12. W. Broniowski, F. Giacosa, and V. Begun, *Phys. Rev.* **C92**, 034905 (2015), arXiv:1506.01260 [nucl-th].



What can we learn from NJL-type models about dense matter?

Michael Buballa

Theoriezentrum, Institut für Kernphysik, TU Darmstadt D-64289 Darmstadt, Germany

Abstract. The merits and limitations of the Nambu–Jona-Lasinio model as a model for strong interactions at nonzero density are critically discussed. We present several examples, demonstrating that, while in general the results should not be trusted quantitatively, the NJL model is a powerful theoretical tool for getting new insights and ideas about the QCD phase diagram and the dense-matter equation of state.

1 Introduction

In 1961, Nambu and Jona-Lasinio published two seminal papers on a “Dynamical Model of Elementary Particles Based on an Analogy with Superconductivity,” [1, 2], now known as the Nambu–Jona-Lasinio (NJL) model. Originally invented as a model for point-like nucleons, after the advent of QCD the NJL model was reinterpreted as a schematic model for quarks, interacting by four-point vertices rather than by the exchange of gluons. Subsequently the model was extended from two to three quark flavors and applied to study effects of nonzero temperature and chemical potential as well as color superconductivity (for reviews, see [3–6]). More recently features of Polyakov-loop dynamics have been added to the model by coupling the quarks to a background temporal gauge field with a phenomenological potential (PNJL model) [7–10].

The ground-breaking achievements of the original NJL papers were to explicitly demonstrate how the spontaneous breaking of chiral symmetry in a quantum-field theoretical context leads to the dynamical generation of fermion masses, while at the same time there appears a massless mode (“Nambu-Goldstone boson”) in the quark-antiquark scattering matrix, which can be identified with the pion. However, despite this indisputable success (culminating in the 2008 Nobel prize awarded to Nambu “for the discovery of the mechanism of spontaneous broken symmetry in subatomic physics”) one may ask why we should still use a model after QCD was established as the theory of the strong interaction. Of course, model calculations are in general much simpler than QCD calculations. But to what extent can we trust the results? In particular we have to face the following problems:

- The essential feature of the NJL model which motivates its use as an effective model of QCD is the fact that the two share the same global symmetries. However, the symmetries alone do not uniquely fix the interaction. There could be

(infinitely) many possible interaction terms, not only containing four-point but also higher $2n$ -point vertices (see, e.g., Ref. [11] and references therein), and thus many parameters.

- In principle, these vertices should be derivable from QCD by integrating out the gluonic degrees of freedom. However, this procedure would lead to density dependent coupling constants, while in actual NJL-model calculations the model parameters are typically fitted to vacuum observables and then kept unchanged in the medium.
- As far as symmetries are concerned, there are model independent theorems, which, if not spoiled by an improper approximation, are reproduced by the model. But those we know anyway while for non-universal properties it is not clear whether the results obtained in the model agree with those in QCD.

In addition, the NJL model has the well-known shortcomings that it is non-renormalizable and has no confinement,¹ which could both lead to artifacts.

There are nevertheless situations where QCD-inspired models in general and specifically the NJL model can be very useful. “Model independent” predictions are sometimes based on unrealistic assumptions, e.g., Taylor expansions in parameters which are not really small. Such cases can be uncovered by specific model calculations. Sometimes models can also be used to test ideas and techniques used in other frameworks. Most importantly, however, models can be employed for exploratory studies in order to identify interesting problems, worthwhile to be studied more seriously.

In the following these statements will be illustrated by specific examples related to the QCD phase diagram and the dense-matter equation of state.

2 Phase diagram at nonzero temperature and density

Despite tremendous theoretical and experimental efforts, the exact phase structure of QCD as a function of temperature and baryon chemical potential $\mu_B \equiv 3\mu$ is still unresolved to a large extent [13, 14]. While at $\mu = 0$ QCD can be solved on the lattice by standard Monte-Carlo methods, this is prevented at $\mu \neq 0$ by the so-called sign problem. Our current picture in this regime is therefore mainly based on model calculations, with the NJL model playing a pioneering role:

In 1989 Asakawa and Yazaki presented an NJL-model calculation of the T - μ phase diagram [15]. At low temperatures but high chemical potential they found a first-order chiral phase transition, while at low μ the transition is a crossover, in agreement with today’s lattice QCD results. As a consequence there is a critical point where the first-order phase boundary ends. Although not much attention was paid to this fact at the beginning, this changed dramatically after it was argued that the critical endpoint (CEP) could have observable consequences [16]. Today the search for the CEP is the main goal of the beam-energy scan at RHIC [17] and of the future projects at NICA [18] and CBM at FAIR [19].

¹ In the PNJL model confinement is *statistically* realized, meaning that the quark contribution to the pressure is suppressed at low temperatures. However, this does not prevent the unphysical decay of mesons into quarks and antiquarks in the model [12].

To my knowledge the NJL-model calculation of Ref. [15] was the first prediction of the CEP. On the other hand, it was already demonstrated in that reference that its exact position depends on the choice of the model parameters. For instance the CEP can be moved around considerably by varying the strength in the vector channel or of the chiral anomaly (parametrized by a six-point interaction in the three-flavor model) [20]. Indeed, already for rather moderate values of the vector coupling, the first-order phase boundary (and hence the CEP) disappears completely.

We can thus conclude that the NJL model (like other models) cannot predict the position of the CEP and not even tell whether it exists. However, it gave the first hint for its possible existence and in this way inspired experimental searches and more serious theoretical investigations. In particular there are now various works which try to identify the CEP directly starting from QCD, both, within functional methods which do not have a sign problem (like truncated Dyson-Schwinger equations [21]) and on the lattice, trying to circumvent the sign problem in some way [22]. For example, one method to get information about the $\mu \neq 0$ regime by lattice calculations is to perform a Taylor expansion of the pressure in powers of μ , evaluating the coefficients at $\mu = 0$. The power of this method can in turn be tested within models which do not have a sign problem and thus allow for a direct comparison of the Taylor-expanded pressure with the exact model results at $\mu \neq 0$. Such test have been performed in the NJL model [23] as well as in the Polyakov-loop extended quark-meson model [24], revealing that the number of expansion coefficients required for the detection of a CEP located at $\mu/T > 1$ would be far beyond the present state of the art.

In most studies of the QCD phase diagram it is tacitly assumed that the chiral condensate, i.e., the order parameter for chiral-symmetry breaking is spatially homogeneous. Allowing for spatially varying condensates, however, it turns out that in the NJL model there is a region where such an inhomogeneous condensate is energetically favored over homogeneous or vanishing condensates [25, 26]. In particular it was found that for the standard NJL Lagrangian the inhomogeneous phase covers the entire first-order phase boundary which is obtained in the case when only homogeneous phases are considered [27]. Moreover, the inhomogeneous phase turned out to be very robust against various model extensions, like including strange quarks [28], isospin asymmetries [29], magnetic fields [30] or, most notably, vector interactions [31] (for a review, see Ref. [32]). Again, the model cannot be used to prove the existence of such phases in QCD, but in the same way as the model prediction of a CEP, the possibility of an inhomogeneous phase should seriously be considered and deserves more thorough investigations. Indeed, inspired by the NJL model results, inhomogeneous phases have also been studied within Dyson-Schwinger QCD, where qualitatively similar results have been found [33].

3 Equation of state for compact stars

Neutron stars can reach densities of several times nuclear-matter densities in their centers. Under these conditions it has been argued long time ago that matter

could be deconfined [34, 35], so that “neutron stars” would in fact be hybrid stars with an outer hadronic part and a quark matter core. Although this idea has been challenged by the recent discovery of two compact stars with masses of about $2M_{\odot}$ (where M_{\odot} is the mass of the sun) [36, 37], the question whether or not there are deconfined quarks at the centers of compact stars is still open [38, 39]. Here the problem is again that QCD at $\mu \neq 0$ cannot be studied on the lattice, and that therefore the QCD equation of state (EoS) at nonzero density is largely unknown. In this situation one often starts from two independent EoSs, a phenomenological hadronic one and a quark-matter one and constructs a phase transition between them by comparing their pressure at given chemical potential.

For the quark-matter part the most common choice are MIT bag-model EoSs, but more recently NJL-model EoSs have also gained popularity. One reason is that the critical chemical potential of the phase transition depends sensitively on the bag constant, which is a largely unconstrained parameter in the bag model, while in the NJL model it is dynamically generated as the pressure difference between the vacuum states with spontaneously broken and unbroken chiral symmetry. Moreover, the NJL model allows for a straightforward incorporation of color superconductivity [6]. Yet, as pointed out earlier, the NJL model has many parameters as well. Indeed, while early studies mostly disfavored the presence of quark matter in neutron stars [40, 41], later analyses succeeded in getting solutions with a quark-matter core, simultaneously reaching maximum masses above $2M_{\odot}$, by choosing relative large couplings in the vector and diquark channels [42]. Hence, the NJL model (in combination with a hadronic model) can serve as a counterexample against the claim that the detection of compact stars with $2M_{\odot}$ already rules out the presence of a quark-matter core [43]. On the other hand, we conclude again that it cannot make qualitative or even quantitative predictions about its existence.

In fact, it is not even clear, whether resorting to the dynamically generated bag pressure of the NJL model really makes sense when combining it with a hadronic model. Basically it means that the NJL model is taken seriously in vacuum and at high densities, but not in the hadronic phase in between. Some authors therefore introduced an additional bag constant by hand, which is supposed to account for confinement effects and other uncertainties [44, 45]. However, it is then even more questionable to fix the NJL-model parameters in vacuum, and one may ask why the NJL model should be used at all. (After all, the most important feature of the NJL model is its nontrivial vacuum.) To my opinion, the only convincing way to ultimately avoid these problems is to describe quark and hadronic phase in a single framework, e.g., construct nucleons and nuclear matter within the NJL model as well. Some steps in this direction have been made in Refs. [46–48]. As an alternative approach it might also be worthwhile to revisit the description of baryons as chiral solitons [49, 50] and investigate their relation to the inhomogeneous phases discussed above.

References

1. Y. Nambu and G. Jona-Lasinio, *Phys. Rev.* **122**, 345 (1961).

2. Y. Nambu and G. Jona-Lasinio, Phys. Rev. **124**, 246 (1961).
3. U. Vogl and W. Weise, Prog. Part. Nucl. Phys. **27**, 195 (1991).
4. S. P. Klevansky, Rev. Mod. Phys. **64**, 649 (1992).
5. T. Hatsuda and T. Kunihiro, Phys. Rept. **247**, 221 (1994).
6. M. Buballa, Phys. Rept. **407**, 205 (2005).
7. P. N. Meisinger and M. C. Ogilvie, Phys. Lett. B **379**, 163 (1996).
8. K. Fukushima, Phys. Lett. B **591**, 277 (2004).
9. E. Megias, E. Ruiz Arriola and L. L. Salcedo, Phys. Rev. D **74**, 065005 (2006).
10. C. Ratti, M. A. Thaler and W. Weise, Phys. Rev. D **73**, 014019 (2006).
11. S. Benic, Eur. Phys. J. A **50**, 111 (2014).
12. H. Hansen, W. M. Alberico, A. Beraudo, A. Molinari, M. Nardi and C. Ratti, Phys. Rev. D **75**, 065004 (2007).
13. P. Braun-Munzinger and J. Wambach, Rev. Mod. Phys. **81**, 1031 (2009).
14. K. Fukushima and T. Hatsuda, Rept. Prog. Phys. **74**, 014001 (2011).
15. M. Asakawa and K. Yazaki, Nucl. Phys. A **504**, 668 (1989).
16. M. A. Stephanov, K. Rajagopal and E. V. Shuryak, Phys. Rev. Lett. **81**, 4816 (1998).
17. G. Odyniec, PoS CPOD **2013**, 043 (2013).
18. D. Blaschke et al., editors, NICA White Paper 10.01 (2014).
19. B. Friman, C. Höhne, J. Knoll, S. Leupold, J. Randrup, R. Rapp and P. Senger, Lect. Notes Phys. **814**, pp.1 (2011).
20. K. Fukushima, Phys. Rev. D **77**, 114028 (2008) Erratum: [Phys. Rev. D **78**, 039902 (2008)].
21. C. S. Fischer, J. Luecker and C. A. Welzbacher, Nucl. Phys. A **931**, 774 (2014).
22. P. de Forcrand, PoS LAT **2009**, 010 (2009).
23. M. Buballa, A. G. Grunfeld, A. E. Radzhabov and D. Scheffler, Prog. Part. Nucl. Phys. **62**, 365 (2009).
24. F. Karsch, B. J. Schaefer, M. Wagner and J. Wambach, Phys. Lett. B **698**, 256 (2011).
25. E. Nakano and T. Tatsumi, Phys. Rev. D **71**, 114006 (2005).
26. D. Nickel, Phys. Rev. Lett. **103**, 072301 (2009).
27. D. Nickel, Phys. Rev. D **80**, 074025 (2009).
28. J. Moreira, B. Hiller, W. Broniowski, A. A. Osipov and A. H. Blin, Phys. Rev. D **89**, no. 3, 036009 (2014).
29. D. Nowakowski, M. Buballa, S. Carignano and J. Wambach, arXiv:1506.04260 [hep-ph].
30. I. E. Frolov, V. C. Zhukovsky and K. G. Klimenko, Phys. Rev. D **82**, 076002 (2010).
31. S. Carignano, D. Nickel and M. Buballa, Phys. Rev. D **82**, 054009 (2010).
32. M. Buballa and S. Carignano, Prog. Part. Nucl. Phys. **81**, 39 (2015).
33. D. Müller, M. Buballa and J. Wambach, Phys. Lett. B **727**, 240 (2013).
34. D. D. Ivanenko and D. F. Kurdgelaidze, Astrophysics **1**, 251 (1965) [Astrofiz. **1**, 479 (1965)].
35. N. Itoh, Prog. Theor. Phys. **44**, 291 (1970).
36. P. Demorest, T. Pennucci, S. Ransom, M. Roberts and J. Hessels, Nature **467**, 1081 (2010).
37. J. Antoniadis *et al.*, Science **340**, 6131 (2013).
38. M. Alford, D. Blaschke, A. Drago, T. Klahn, G. Pagliara and J. Schaffner-Bielich, Nature **445**, E7 (2007).
39. M. Buballa *et al.*, J. Phys. G **41**, no. 12, 123001 (2014).
40. K. Schertler, S. Leupold and J. Schaffner-Bielich, Phys. Rev. C **60**, 025801 (1999).
41. M. Baldo, M. Buballa, F. Burgio, F. Neumann, M. Oertel and H. J. Schulze, Phys. Lett. B **562**, 153 (2003).
42. T. Klahn, D. Blaschke, F. Sandin, C. Fuchs, A. Faessler, H. Grigorian, G. Röpke and J. Trümper, Phys. Lett. B **654**, 170 (2007).

43. F. Özel, *Nature* **441**, 1115 (2006).
44. G. Pagliara and J. Schaffner-Bielich, *Phys. Rev. D* **77**, 063004 (2008).
45. C. H. Lenzi and G. Lugones, *Astrophys. J.* **759** (2012) 57.
46. A. H. Rezaeian and H. J. Pirner, *Nucl. Phys. A* **769**, 35 (2006).
47. S. Lawley, W. Bentz and A. W. Thomas, *J. Phys. G* **32**, 667 (2006).
48. J. c. Wang, Q. Wang and D. H. Rischke, *Phys. Lett. B* **704**, 347 (2011).
49. R. Alkofer, H. Reinhardt and H. Weigel, *Phys. Rept.* **265**, 139 (1996).
50. C. V. Christov, A. Blotz, H. C. Kim, P. Pobylytsa, T. Watabe, T. Meissner, E. Ruiz Arriola and K. Goeke, *Prog. Part. Nucl. Phys.* **37**, 91 (1996).



The Sign Problem in QCD

Thomas D. Cohen

Department of Physics, University of Maryland, College Park, MD 20742-4111



The microscopic structure of πNN , $\pi N\Delta$ and $\pi\Delta\Delta$ vertices in a hybrid constituent quark model*

Ju-Hyun Jung and Wolfgang Schweiger

Institute of Physics, University of Graz, A-8010 Graz, Austria

Abstract. We present a microscopic description of the strong πNN , $\pi N\Delta$ and $\pi\Delta\Delta$ vertices. Our starting point is a constituent-quark model supplemented by an additional $3q\pi$ non-valence component. In the spirit of chiral constituent-quark models, quarks are allowed to emit and reabsorb a pion. This multichannel system is treated in a relativistically invariant way within the framework of point-form quantum mechanics. Starting with a common $SU(6)$ spin-flavor-symmetric wave function for N and Δ , we calculate the strength of the πNN , $\pi N\Delta$ and $\pi\Delta\Delta$ couplings and the corresponding vertex form factors. Our results are in accordance with phenomenological fits of these quantities that have been obtained within purely hadronic multichannel models for baryon resonances.

1 Introduction

One of the big deficiencies of conventional constituent-quark models is the fact that all states come out as stable bound states. In nature, however, excited states are rather resonances with a finite decay width. In order to remedy this situation, we study a constituent-quark model with explicit pionic degrees of freedom. The underlying physics is that of “chiral constituent-quark models”. This means that the spontaneous chiral-symmetry breaking of QCD produces pions as the associated Goldstone bosons and constituent quarks as effective particles [1], with the pions coupling directly to the constituent quarks. The occurrence of pions affects then the masses and the structure of the hadrons and leads to resonance-like behavior of hadron excitations. If one assumes instantaneous confinement between the quarks, only “bare” hadrons, i.e. eigenstates of the pure confinement problem, can propagate. As a consequence, pionic effects on hadron masses and structure can be formulated as a purely hadronic problem with the hadron substructure entering pion-hadron vertex form factors¹. In the present contribution we will present predictions for πNN , $\pi N\Delta$ and $\pi\Delta\Delta$ couplings and vertex form factors, given the πqq coupling and an $SU(6)$ spin-flavor symmetric model for the $3q$ wave function of the nucleon and the Δ .

* Talk delivered by Ju-Hyun Jung

¹ Strictly speaking these are vertex form factors of the bare hadrons.

2 Formalism

Our starting point for calculating the strong πNN , $\pi N\Delta$ and $\pi\Delta\Delta$ couplings and form factors is the mass-eigenvalue problem for 3 quarks that are confined by an instantaneous potential and can emit and reabsorb a pion. To describe this system in a relativistically invariant way, we make use of the point-form of relativistic quantum mechanics. Employing the Bakamjian-Thomas construction, the overall 4-momentum operator \hat{P}^μ can be separated into a free 4-velocity operator \hat{V}^μ and an invariant mass operator \hat{M} that contains all the internal motion, i.e. $\hat{P}^\mu = \hat{M}\hat{V}^\mu$ [2]. Bakamjian-Thomas-type mass operators are most conveniently represented by means of velocity states $|V; \mathbf{k}_1, \mu_1; \mathbf{k}_2, \mu_2; \dots; \mathbf{k}_n, \mu_n\rangle$, which specify the system by its overall velocity V ($V_\mu V^\mu = 1$), the CM momenta \mathbf{k}_i of the individual particles and their (canonical) spin projections μ_i [2]. Since the physical baryons of our model contain, in addition to the $3q$ -component, also a $3q\pi$ -component, the mass eigenvalue problem can be formulated as a 2-channel problem of the form

$$\begin{pmatrix} \hat{M}_{3q}^{\text{conf}} & \hat{K}_\pi \\ \hat{K}_\pi^\dagger & \hat{M}_{3q\pi}^{\text{conf}} \end{pmatrix} \begin{pmatrix} |\psi_{3q}\rangle \\ |\psi_{3q\pi}\rangle \end{pmatrix} = m \begin{pmatrix} |\psi_{3q}\rangle \\ |\psi_{3q\pi}\rangle \end{pmatrix}, \quad (1)$$

with $|\psi_{3q}\rangle$ and $|\psi_{3q\pi}\rangle$ denoting the two Fock-components of the physical baryon states $|B\rangle$. The mass operators on the diagonal contain, in addition to the relativistic particle energies, an instantaneous confinement potential between the quarks. The vertex operator \hat{K}_π^\dagger connects the two channels and describes the absorption (emission) of the π by one of the quarks. Its velocity-state representation can be directly connected to a corresponding field-theoretical interaction Lagrangean [2]. We use a pseudovector interaction Lagrangean for the πqq -coupling

$$\mathcal{L}_{\pi qq}(x) = -\frac{f_{\pi qq}}{m_\pi} (\bar{\psi}_q(x) \gamma_\mu \gamma_5 \boldsymbol{\tau} \psi_q(x)) \cdot \partial^\mu \boldsymbol{\phi}_\pi(x), \quad (2)$$

where the “ \cdot ”-product has to be understood as product in isospin space. After elimination of the $3q\pi$ -channel the mass-eigenvalue equation takes on the form

$$\left[\hat{M}_{3q}^{\text{conf}} + \underbrace{\hat{K}_\pi (m - \hat{M}_{3q\pi}^{\text{conf}})^{-1} \hat{K}_\pi^\dagger}_{\hat{V}_\pi^{\text{opt}}(m)} \right] |\psi_{3q}\rangle = m |\psi_{3q}\rangle, \quad (3)$$

where $\hat{V}_\pi^{\text{opt}}(m)$ is an optical potential that describes the emission and reabsorption of the pion by the quarks. One can now solve Eq. (3) by expanding the ($3q$ -components of the) eigenstates in terms of eigenstates of the pure confinement problem, i.e. $|\psi_{3q}\rangle = \sum_{B_0} \alpha_{B_0} |B_0\rangle$, and determining the open coefficients α_{B_0} . Since the particles which propagate within the pion loop are also bare baryons (rather than quarks), the problem of solving the mass eigenvalue equation (3) reduces then to a pure hadronic problem, in which the dressing and mixing of bare baryons by means of pion loops produces finally the physical baryons (see Fig. 1). As also indicated in Fig. 1, the quark substructure determines just the coupling strengths at the pion-baryon vertices and leads to vertex form factors. To set up

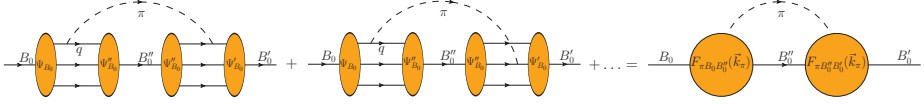


Fig. 1. Graphical representation of the kernel $\langle B'_0 | \hat{V}_\pi^{\text{opt}}(m) | B_0 \rangle$ needed to solve the mass-eigenvalue equation (3).

the mass-eigenvalue equation on the hadronic level one needs matrix elements $\langle B'_0 | \hat{V}_\pi^{\text{opt}}(m) | B_0 \rangle$ of the optical potential between bare baryon (velocity²) states. The general structure of these matrix elements is (B_0 and B'_0 are at rest)

$$\langle B'_0 | \hat{V}_\pi^{\text{opt}}(m) | B_0 \rangle \propto \sum_{B''_0} \int \frac{d^3 \mathbf{k}''_\pi}{2\sqrt{m_\pi^2 + \mathbf{k}''_\pi{}^2}} J_{\pi B''_0 B'_0}^{5*}(\mathbf{k}''_\pi) \frac{1}{m - m_{B''_0 \pi}} J_{\pi B''_0 B_0}^5(\mathbf{k}''_\pi), \quad (4)$$

where $m_{B''_0 \pi}$ is the invariant mass of the $B''_0 \pi$ system in the intermediate state and spin- as well as isospin dependencies have been suppressed.

For the cases we are interested in, i.e. the N and the Δ , the currents occurring in Eq. (4) can be cast into the form³:

$$\begin{aligned} J_{\pi N_0 N_0}^5(\mathbf{k}_\pi) &= i \frac{f_{\pi N_0 N_0}}{m_\pi} F_{\pi N_0 N_0}(\mathbf{k}_\pi^2) \bar{u}(-\mathbf{k}_\pi) \gamma_\mu \gamma_5 u(\mathbf{0}) k_\pi^\mu, \\ J_{\pi \Delta_0 \Delta_0}^5(\mathbf{k}_\pi) &= \frac{f_{\pi \Delta_0 \Delta_0}}{m_\pi m_{\Delta_0}} F_{\pi \Delta_0 \Delta_0}(\mathbf{k}_\pi^2) \epsilon^{\mu\nu\rho\sigma} \bar{u}_\mu(-\mathbf{k}_\pi) u_\nu(\mathbf{0}) k_{\Delta_0, \rho} k_{\pi, \sigma}, \\ J_{\pi N_0 \Delta_0}^5(\mathbf{k}_\pi) &= -i \frac{f_{\pi N_0 \Delta_0}}{m_\pi m_{\Delta_0}} F_{\pi N_0 \Delta_0}(\mathbf{k}_\pi^2) \epsilon^{\mu\nu\rho\sigma} \bar{u}(-\mathbf{k}_\pi) \gamma_\sigma \gamma_5 u_\nu(\mathbf{0}) k_{\Delta_0, \mu} k_{\pi, \rho}, \\ J_{\pi \Delta_0 N_0}^5(\mathbf{k}_\pi) &= i \frac{f_{\pi N_0 \Delta_0}}{m_\pi m_{\Delta_0}} F_{\pi \Delta_0 N_0}(\mathbf{k}_\pi^2) \epsilon^{\mu\nu\rho\sigma} \bar{u}_\nu(-\mathbf{k}_\pi) \gamma_5 \gamma_\sigma u(\mathbf{0}) k_{\Delta_0, \mu} k_{\pi, \rho}, \end{aligned} \quad (5)$$

where $u(\cdot)$ is the Dirac spinor of the nucleon and $u_\mu(\cdot)$ the Rarita-Schwinger spinor of the Δ . Here we have again suppressed the isospin dependence and also omitted the spin labels. From Eqs. (4) and (5) one can then infer the analytical expression for the combination $f_{\pi B'_0 B_0} F_{\pi B'_0 B_0}(\mathbf{k}_\pi^2)$ in terms of quark degrees of freedom. It is an integral over the (independent) quark momenta involving the $3q$ wave function of the in- and outgoing (bare) baryons, the pseudovector quark current as resulting from the Lagrangean (2) and some kinematical as well as Wigner-rotation factors [4].

Assuming a scalar isoscalar confinement potential, the masses of the bare nucleon and the bare Δ are degenerate, the momentum part of the wave function will be the same and the spin-flavor part of the wave function is $SU(6)$ symmetric. Rather than solving the confinement problem for a particular potential, we thus

² We suppress this velocity dependence since it factors out and has no influence on the mass spectrum.

³ Note that this form exhibits the correct chiral properties and avoids problems with superfluous spin degrees of freedom when treating spin-3/2 fields covariantly by means of Rarita-Schwinger spinors [3].

parameterize the momentum part of the $3q$ wave function of N_0 and Δ_0 by means of a Gaussian

$$\psi_{3q}^{N_0, \Delta_0}(\mathbf{k}_{q_1}, \mathbf{k}_{q_2}, \mathbf{k}_{q_3}) \propto \exp(-\alpha^2(\mathbf{k}_{q_1}^2 + \mathbf{k}_{q_2}^2 + \mathbf{k}_{q_3}^2)), \quad \mathbf{k}_{q_1} + \mathbf{k}_{q_2} + \mathbf{k}_{q_3} = \mathbf{0}, \quad (6)$$

and choose an appropriate value for the mass of N_0 and Δ_0 , i.e. $M_{N_0} = M_{\Delta_0} =: M_0$. The parameters of our model are therefore the oscillator parameter α , the N_0 and Δ_0 mass M_0 , the constituent-quark mass $m_q := m_u = m_d$ and $f_{\pi qq}$, the πqq coupling strength. For fixed $m_q = 263$ MeV we have adapted the remaining parameters such that the physical N and Δ masses, resulting from the mass renormalization due to pion loops (with N_0 and Δ_0 intermediate states), agree with their experimental values. This gives us for the remaining parameters $M_0 = 1.552$ GeV, $\alpha = 2.56$ GeV $^{-1}$ and $f_{\pi qq} = 0.6953$.

3 Results and Outlook

Having fixed the parameters of our model, we are now able to make predictions for the strong $\pi N_0 N_0$, $\pi \Delta_0 \Delta_0$, $\pi N_0 \Delta_0$, and $\pi \Delta_0 N_0$ couplings and form factors. The top plot of Fig. 2 shows these (unnormalized) form factors as function of the (negative) four-momentum transfer squared (analytically continued to small time-like momentum transfers). It is worth noting that $F_{\pi \Delta_0 N_0}$ and $F_{\pi N_0 \Delta_0}$ do not agree. This is, of course, no surprise, since in the first case the N_0 is real and the Δ_0 virtual, whereas it is just the other way round in the second case. The form factors describe thus completely different kinematical situations, but they coincide at a particular negative (i.e. unphysical) value of Q^2 . Since there is only one coupling strength at the $\pi N_0 \Delta_0$ -vertex (i.e. $f_{\pi \Delta_0 N_0} = f_{\pi N_0 \Delta_0}$, see Eq. (5)), this is the natural point to normalize the form factors and extract the coupling constants. Its value $Q_0^2 = -0.090$ GeV 2 is close to the standard normalization point, namely the pion pole $Q_0^2 = -m_\pi^2$. Comparing the resulting coupling strengths, we get the ratio $f_{\pi N_0 \Delta_0} : f_{\pi N_0 N_0} : f_{\pi \Delta_0 \Delta_0} = 1.208 : 1 : 0.608$. This should be compared with the prediction from the non-relativistic constituent-quark model assuming SU(6) spin-flavor symmetry, i.e. $f_{\pi N \Delta} : f_{\pi N N} : f_{\pi \Delta \Delta} = 4\sqrt{2}/5 : 1 : 4/5 = 1.13 : 1 : 0.8$ [8]. The differences can solely be ascribed to relativistic effects and are obviously significant, in particular for the $\pi \Delta_0 \Delta_0$ -vertex. Remarkably, our results resemble very much those needed in dynamical coupled-channel models, e.g. $f_{\pi N \Delta} : f_{\pi N N} : f_{\pi \Delta \Delta} = 1.26 : 1 : 0.42$ in Ref. [6].

In the bottom plot of Fig. 2 our result for $F_{\pi N_0 N_0}$ is compared with the outcome of another relativistic constituent-quark model [5] and with two parameterizations of this form factor that have been used in dynamical coupled-channel models [6, 7]. Up to $Q^2 \approx 1$ GeV 2 our prediction is comparable with the form factor parametrization of Ref. [7], but for higher Q^2 it falls off slower. The form factors of Refs. [5, 6] fall off much faster already at small Q^2 . Deviations of our result from the one of Ref. [5] have their origin in different $3q$ wave functions of the nucleon, but also in different kinematical and spin-rotation factors entering the microscopic expression for the pseudovector current of the nucleon.

Having determined the $\pi N_0 N_0$, $\pi \Delta_0 \Delta_0$ and $\pi N_0 \Delta_0$ vertices from a microscopic model, we are now in the position to calculate the electromagnetic form

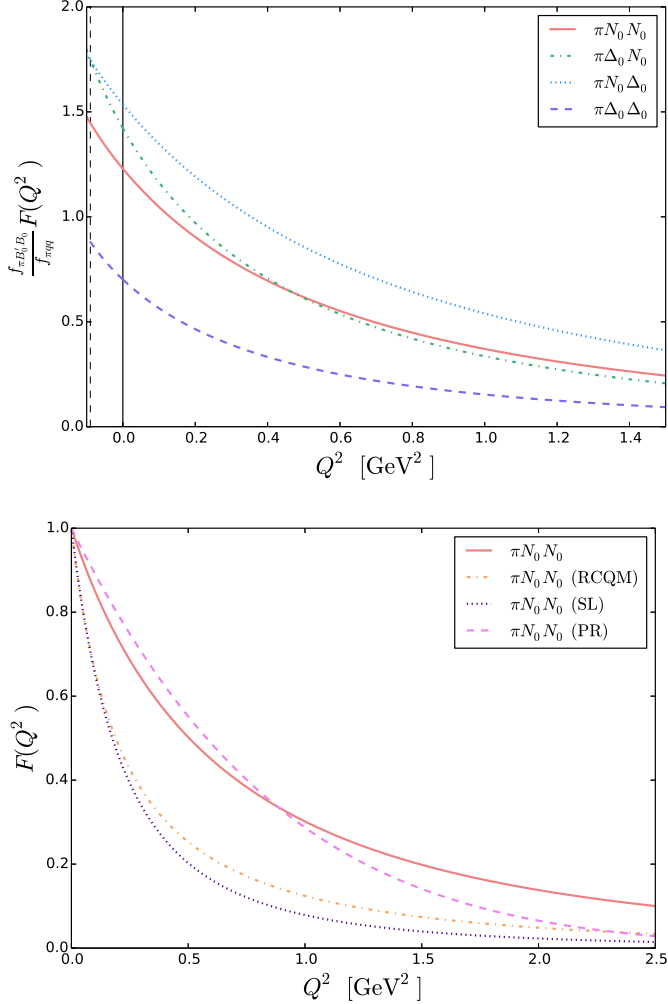


Fig. 2. The top plot shows the (unnormalized) $\pi N_0 N_0$, $\pi \Delta_0 \Delta_0$, $\pi N_0 \Delta_0$, and $\pi \Delta_0 N_0$ form factors as functions of $Q^2 = -2M_0(M_0 - (M_0^2 + \mathbf{k}_\pi^2)^{1/2})$. In the bottom plot the Q^2 behavior of $F_{\pi N_0 N_0}$ (normalized to 1 at $Q^2 = 0$) is compared to the outcome of another relativistic constituent-quark model (RCQM) [5] and of phenomenological fits obtained within two purely hadronic dynamical coupled-channel models [6,7] (SL and PR).

factors of physical nucleons and Deltas and determine the effect of pions on their electromagnetic structure. First exploratory calculations for the nucleon show that visible effects can be expected for $Q^2 \lesssim 0.5 \text{ GeV}^2$ [4]. It will, of course, be more interesting to investigate electromagnetic Δ and $N \rightarrow \Delta$ transition form factors, where pionic effects are expected to play a more significant role.

References

1. L. Y. Glozman and D. O. Riska, Phys. Rept. **268**, 263 (1996)
2. E. P. Biernat, W. H. Klink and W. Schweiger, Few Body Syst. **49**, 149 (2011)
3. V. Pascalutsa, and M. Vanderhaeghen, Phys. Lett. B **636**, 31 (2006)
4. D. Kupelwieser, Ph.D. thesis, University of Graz (2016)
5. T. Melde, L. Canton, and W. Plessas, Phys. Rev. Lett. **102**, 132002 (2009)
6. H. Kamano, S. X. Nakamura, T.-S. H. Lee, and T. Sato, Phys. Rev. C **88**, 035209 (2013)
7. H. Polinder and T. A. Rijken, Phys. Rev. C **72**, 065211 (2005)
8. G. E. Brown and W. Weise, Phys. Rept. **22**, 279 (1975)



The nucleon spin in deep inelastic scattering

Bogdan Povh

Max-Planck-Institut für Kernphysik, Postfach 103980, D-69029 Heidelberg, Germany

The following conflict has been pointed out. In the **constituent quark model** with constituent quarks containing a pion cloud [1] the value of quark spin content amounts to $\Delta\Sigma \approx 0.6$. In the evaluation of the **deep inelastic scattering (DIS)** [2,3], however, the value $\Delta\Sigma \approx 0.33$ is quoted. Possible resolutions of this conflict have been discussed.

References

1. M. Rosina and B. Povh, Bled Workshops in Physics **14** (2013) No.1, 52-56; also available at <http://www-f1.ijs.si/BledPub>.
2. K. Rith, Prog. Part. Nucl. Phys. **49** (2002) 245.
3. A. Airapetian et al., Phys. Rev. D **75** (2007) 012007.



Angular momentum content of the $\rho(1450)$ from chiral lattice fermions*

C. Rohrhofer, M. Pak, L. Ya. Glozman

Institut für Physik, FB Theoretische Physik, Universität Graz, Universitätsplatz 5, 8010 Graz, Austria

Abstract. We identify the chiral and angular momentum content for the leading quark-antiquark Fock component for the $\rho(770)$ and $\rho(1450)$ mesons using a lattice simulation with chiral fermions. Our analysis shows that in the angular momentum basis the $\rho(770)$ is a 3S_1 state, in accordance with the quark model. The $\rho(1450)$ is a 3D_1 state, showing that the quark model wrongly assumes the $\rho(1450)$ to be a radial excitation of the $\rho(770)$.

1 Introduction

An interesting question in hadronic physics is the origin of spin and distribution of angular momentum. How the spin of a hadron is generated, and by which constituents it is carried, is a priori not clear. In the non-relativistic, constituent quark model [2], which has been quite successful in delivering a classification scheme for the low-lying hadron spectrum, the spin of a hadron is assigned solely to its valence quarks. Being an effective classification scheme, it does not care about foundations in terms of underlying QCD dynamics. Despite its successes the non-relativistic description clearly has limitations.

In this project we investigate the angular momentum content of the $\rho(770)$ and $\rho(1450)$ mesons. In the spectroscopic notation $n^{2S+1}L_J$ the $\rho(770)$ is assigned to the 1^3S_1 state by the quark model. The $\rho(1450)$ is assigned to the 2^3S_1 state, hence being the first radial excitation of the $\rho(770)$. However, this assumption is by far not clear from the underlying QCD dynamics, and is an output of the non-relativistic potential description of a meson as a two-body system.

The angular momentum content of the leading quark-antiquark Fock components of mesons can in principle be identified by lattice simulations. Studies like [3], which rely on heavy quarks for the non-relativistic reduction of hadrons, find good agreement with the quark model classification. However, there is an alternative approach to project non-perturbative lattice results onto the quark model assuming ultra-relativistic quarks. Latter method, which is explained and has been applied in previous studies [4–8], makes use of the chiral-parity group and an unitary transformation to the $^{2S+1}L_J$ basis.

Main ingredients to such an investigation are the overlap factors of operators obtained in lattice calculations. In our study it is crucial that these operators

* Talk delivered by C. Rohrhofer

form a complete set with respect to the chiral-parity group. From these overlap factors the chiral content of a state can be identified, and using the unitary transformation also the angular momentum content. Since the chiral properties are important for such a study, we need a proper lattice fermion discretization, which respects chiral symmetry. For this purpose we use overlap fermions, which distinguishes the present study from the previous ones.

2 Method and Simulation

The full details of this study, its methodology and simulation parameters, can be found in the main paper [1] and references therein. Here we present the idea and summarize the most important components.

To generate states with ρ quantum numbers $(1, 1^{--})$ two different local interpolators can be used, which belong to two distinct chiral representations

$$J_\rho^V(x) = \bar{\Psi}(x)(\tau^a \otimes \gamma^i)\Psi(x) \in (0, 1) \oplus (1, 0) \quad (1)$$

$$J_\rho^T(x) = \bar{\Psi}(x)(\tau^a \otimes \gamma^0 \gamma^i)\Psi(x) \in (1/2, 1/2)_b. \quad (2)$$

We denote them according to their Dirac structure as *vector* (V) and *pseudotensor* (T) interpolators. In a next step we connect the chiral basis to the angular momentum basis with quantum numbers isospin I and $^{2S+1}l_J$. For spin-1 isovector mesons there are only two allowed states $|1;^3S_1\rangle$ and $|1;^3D_1\rangle$, which are connected to the chiral basis by a unitary transformation:

$$|\rho_{(0,1) \oplus (1,0)}\rangle = \sqrt{\frac{2}{3}} |1;^3S_1\rangle + \sqrt{\frac{1}{3}} |1;^3D_1\rangle, \quad (3)$$

$$|\rho_{(1/2,1/2)_b}\rangle = \sqrt{\frac{1}{3}} |1;^3S_1\rangle - \sqrt{\frac{2}{3}} |1;^3D_1\rangle. \quad (4)$$

Note that the operators (1),(2) form a complete and orthogonal basis with respect to the chiral group. Through the unitary transformation (3),(4) they also form a complete and orthogonal basis with respect to the angular momentum content.

On the lattice we evaluate the correlators $\langle J(t)J^\dagger(0) \rangle$. We apply the variational technique, where different interpolators are used to construct the correlation matrix $\langle J_l(t)J_m^\dagger(0) \rangle = C(t)_{lm}$. By solving the generalized eigenvalue problem

$$C(t)_{lm} u_m^{(n)} = \lambda^{(n)}(t, t_0) C(t_0)_{lm} u_m^{(n)} \quad (5)$$

the masses of states can be extracted in a standard way. Denoting $\alpha_l^{(n)} = \langle 0 | J_l | n \rangle$ as the overlap of interpolator J_l with the physical state $|n\rangle$, the relative weight of the chiral representations is now given by

$$\frac{C(t)_{lj} u_j^{(n)}}{C(t)_{kj} u_j^{(n)}} = \frac{\alpha_l^{(n)}}{\alpha_k^{(n)}}. \quad (6)$$

We can extract the ratio α_V/α_T for each state n . Then via the unitary transformation (3),(4) we arrive at the angular momentum content of the ρ mesons.

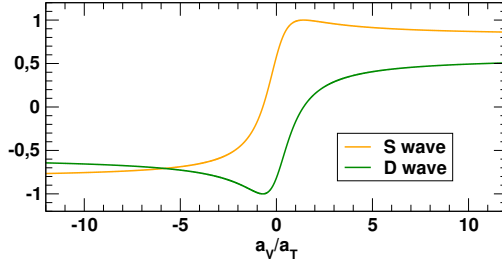


Fig. 1. Partial wave content of ρ mesons in dependence of the relative chiral contribution a_V/a_T , which are connected via transformation (3),(4).

For any lattice simulation an intrinsic resolution scale is set by the lattice spacing a . This means that probing the hadron structure with point-like sources gives results at a scale fixed by the ultraviolet regularization a .

In order to measure the structure close to the infrared region we introduce a different resolution scale by smearing the sources of the quark propagators. We use four different smearing widths in this study. The radius σ of a given source $S(x; x_0)$ is calculated by

$$\sigma^2 = \frac{\sum_x (x - x_0)^2 |S(x; x_0)|^2}{\sum_x |S(x; x_0)|^2}, \quad (7)$$

where we define the resolution scale as $R = 2\sigma$. The smeared profiles of the sources used in this study are pictured in Figure 2. The *Ultra Wide* source does not resolve details smaller than ~ 0.9 fm and marks our infrared end, where we ultimately extract the resolution scale dependent quantities.

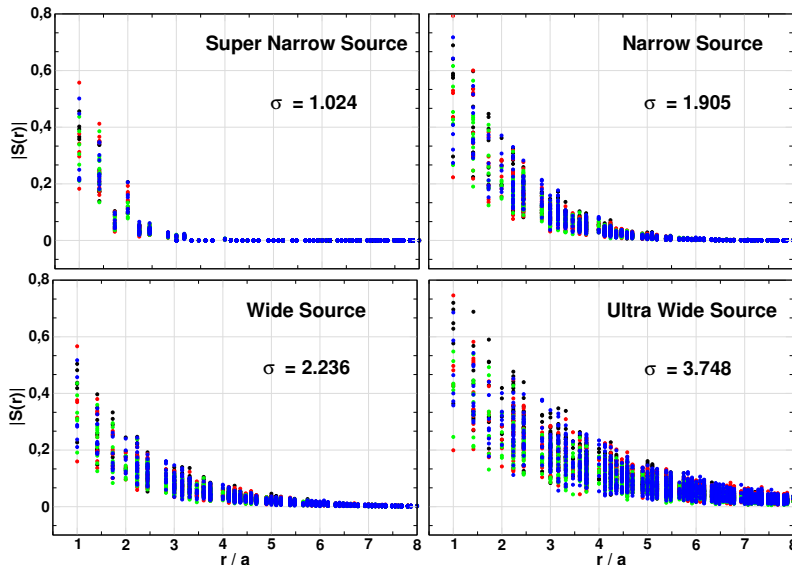


Fig. 2. Different source profiles. σ is their radius in lattice units.

3 Results

To study the ratio a_V/a_T at different resolution scales R we solve the eigenvalue problem (5) with operators (1) and (2) and four different smearings. Then using (6) we extract the ratio a_V/a_T as a function of R . In Fig. 4 we show the ratio a_V/a_T at different resolution scales R . We find a clear R -effect for the ratio a_V/a_T : both ρ and ρ' states are linear dependent on the resolution scale.

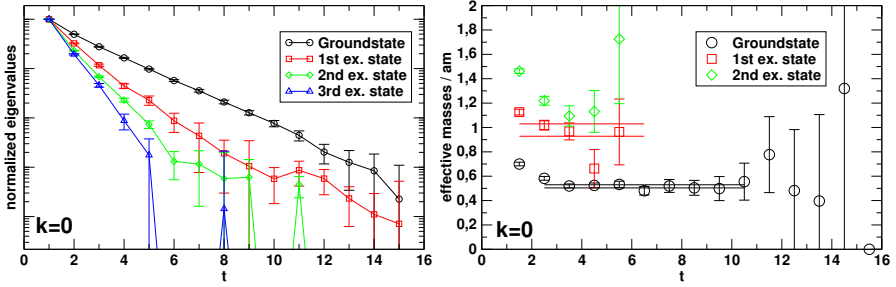


Fig. 3. Normalized eigenvalues and effective masses.

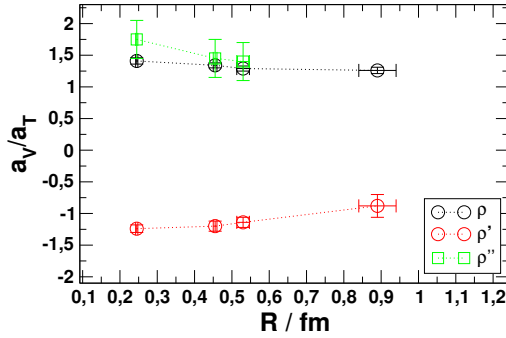


Fig. 4. a_V/a_T ratio for different resolutions.

Using now transformations (3),(4) we find:

$$|\rho(770)\rangle = + (0.998 \pm 0.002) |^3S_1\rangle - (0.05 \pm 0.025) |^3D_1\rangle, \quad (8)$$

$$|\rho(1450)\rangle = - (0.106 \pm 0.09) |^3S_1\rangle - (0.994 \pm 0.005) |^3D_1\rangle. \quad (9)$$

$$|\rho(1700)\rangle = + (0.99 \pm 0.01) |^3S_1\rangle - (0.01 \pm 0.12) |^3D_1\rangle. \quad (10)$$

The ground state ρ is therefore practically a pure 3S_1 state, in agreement with the potential quark model assumption.

The first excited ρ is, however, a 3D_1 state with a very small admixture of a 3S_1 wave. The second excited state is almost pure 3S_1 state. The latter results are in clear contradiction with the potential constituent quark model that attributes the first excited state of the ρ -meson to a radially excited 3S_1 state and the next excited state to a 3D_1 state.

Acknowledgments

The speaker wishes to thank the organizers for the warm welcome and hospitality during the workshop. We thank the JLQCD collaboration for supplying us with the Overlap gauge configurations, M. Denissenya and C.B. Lang for discussions and help. The calculations have been performed on local clusters at ZID at the University of Graz and the Graz University of Technology. Support from the Austrian Science Fund (FWF) through the grants DK W1203-N16 and P26627-N27 is acknowledged.

References

1. C. Rohrhofer, M. Pak and L. Y. Glozman, arXiv:1603.04665 [hep-lat].
2. K. A. Olive *et al.* [Particle Data Group Collaboration], Chin. Phys. C **38** (2014) 090001. doi:10.1088/1674-1137/38/9/090001
3. J. J. Dudek, Phys. Rev. D **84** (2011) 074023 doi:10.1103/PhysRevD.84.074023 [arXiv:1106.5515 [hep-ph]].
4. L. Y. Glozman, C. B. Lang and M. Limmer, Phys. Rev. Lett. **103**, 121601 (2009) doi:10.1103/PhysRevLett.103.121601 [arXiv:0905.0811 [hep-lat]].
5. L. Y. Glozman, C. B. Lang and M. Limmer, Few Body Syst. **47** (2010) 91 [arXiv:0909.2939 [hep-lat]].
6. L. Y. Glozman, C. B. Lang and M. Limmer, Phys. Rev. D **82**, 097501 (2010) doi:10.1103/PhysRevD.82.097501 [arXiv:1007.1346 [hep-lat]].
7. L. Y. Glozman, C. B. Lang and M. Limmer, Phys. Lett. B **705** (2011) 129 [arXiv:1106.1010 [hep-ph]].
8. L. Y. Glozman, C. B. Lang and M. Limmer, Prog. Part. Nucl. Phys. **67** (2012) 312 [arXiv:1111.2562 [hep-ph]].



Excited hyperons of the $N = 2$ band in the $1/N_c$ expansion

Fl. Stancu

University of Liège, Institute of Physics B5, Sart Tilman, B-4000 Liège 1, Belgium

Abstract. The spectrum of excited baryons in the $N = 2$ band is reanalyzed in the $1/N_c$ expansion method, with emphasis on hyperons. Predictions are made for the classification of these excited baryons into $SU(3)$ singlets, octets and decuplets.

1 Introduction

The $1/N_c$ expansion method [1,2] where N_c is the number of colors, is a powerful and systematic tool for baryon spectroscopy. For N_f flavors, the ground state baryons display an exact contracted $SU(2N_f)$ spin-flavor symmetry in the large N_c limit of QCD [3,4]. The Skyrme model, the strong coupling theory and the static quark model share a common underlying symmetry with QCD baryons in the large N_c limit [5].

The method has been successfully applied to ground state baryons ($N = 0$ band), in the symmetric representation **56** of $SU(6)$ [4,6–9]. At $N_c \rightarrow \infty$ the ground state baryons are degenerate. At large, but finite N_c , the mass splitting starts at order $1/N_c$ as first observed in Ref. [5].

The extension of the $1/N_c$ expansion method to excited states requires the symmetry group $SU(2N_f) \times O(3)$ [10], in order to introduce orbital excitations. It happens that the experimentally observed resonances can approximately be classified as $SU(2N_f) \times O(3)$ multiplets, grouped into excitation bands, $N = 1, 2, 3, \dots$, each band containing a number of $SU(6) \times O(3)$ multiplets.

The situation is technically more complicated for mixed symmetric states than for symmetric states. Two approaches have been proposed so far. The first one is based on the Hartree approximation and describes the N_c quark system as a ground state symmetric core of $N_c - 1$ quarks and an excited quark [11].

The second procedure, where the Pauli principle is implemented to all N_c identical quarks has been proposed in Refs. [12,13]. There is no physical reason to separate the excited quark from the rest of the system. The method can straightforwardly be applied to all excitation bands. It requires the knowledge of the matrix elements of all the $SU(2N_f)$ generators acting on mixed symmetric states described by the partition $(N_c - 1, 1)$. In both cases the mass splitting starts at order N_c^0 . The latest achievements for the ground state and the current status of large N_c QCD excited baryons ($N = 1, 2, 3, 4$) can be found in Ref. [14]. The N

= 1 band is the most studied. The $N = 2$ band received considerable attention too. Here we reanalyze the results of Ref. [15] for $N = 2$. The reason is that in a few octets an anomalous situation appeared where the hyperons Λ or Σ (presently degenerate) appeared slightly lighter than the nucleon in the same octet.

Here we use the data of the 2014 Particle Data Group [16] which includes changes due to a more complex analysis of all major photo-production of mesons in a coupled-channel partial wave analysis.

2 The Mass Operator

The general form of the mass operator, where the $SU(3)$ symmetry is broken, has first been proposed in Ref. [9] as

$$M = \sum_i c_i O_i + \sum_i d_i B_i. \quad (1)$$

The operators O_i are defined as the scalar products

$$O_i = \frac{1}{N_c^{n-1}} O_\ell^{(k)} \cdot O_{SF}^{(k)}, \quad (2)$$

where $O_\ell^{(k)}$ is a k -rank tensor in $SO(3)$ and $O_{SF}^{(k)}$ a k -rank tensor in $SU(2)$ -spin, but invariant in $SU(N_f)$. Thus O_i is rotational invariant. For the ground state one has $k = 0$. The excited states also require $k = 1$ and $k = 2$ terms. The $k = 1$ tensor has three components, which are the generators L^i of $SO(3)$. The components of the $k = 2$ tensor operator of $SO(3)$ read

$$L^{(2)ij} = \frac{1}{2} \{L^i, L^j\} - \frac{1}{3} \delta_{i,-j} L \cdot L. \quad (3)$$

The operators $O_{SF}^{(k)}$ are expressed in terms of the $SU(N_f)$ generators S^i , T^a and G^{ia} .

The operators B_i break the $SU(3)$ flavor symmetry and are defined to have zero expectation values for nonstrange baryons. The coefficients c_i encode the quark dynamics and d_i measure the $SU(3)$ breaking. They are obtained from a numerical fit. The most dominant operators considered in the mass formula together with the fitted coefficients are presented in Table 1.

For the [56]-plets the spin-orbit operator O_2 is defined in terms of angular momentum L^i components acting on the whole system as in Ref. [17] and is order $\mathcal{O}(1/N_c)$

$$O_2 = \frac{1}{N_c} L \cdot S, \quad (4)$$

while for the [70]-plets it is defined as a single-particle operator $\ell \cdot s$ of order $\mathcal{O}(N_c^0)$.

$$O_2 = \ell \cdot s = \sum_{i=1}^{N_c} \ell(i) \cdot s(i). \quad (5)$$

3 Matrix elements

The matrix elements of the $[56, 2^+]$ multiplet were derived in Ref. [17]. Details of the derivation of the matrix elements of O_i for $[70, \ell^+]$, as a function of N_c , can be found in Ref. [18]. Note that in the case of mixed symmetric states the matrix elements of O_6 are $\mathcal{O}(N_c^0)$, in contrast to the symmetric case where they are $\mathcal{O}(N_c^{-1})$, and non-vanishing only for octets, while for the symmetric case they are non-vanishing for decuplets. Thus, at large N_c the splitting starts at order $\mathcal{O}(N_c^0)$ for mixed symmetric states due both to O_2 and O_6 .

The SU(3) flavor breaking operators B_i have the same definition for both the symmetric and mixed symmetric multiplets. The matrix elements of B_2 and B_3 for $[70, \ell^+]$ were first calculated in Ref. [15]. For practical purposes we have summarized these results by two simple analytic formulas valid at $N_c = 3$. The diagonal matrix elements of B_2 take the following form

$$B_2 = -n_s \frac{\langle L \cdot S \rangle}{6\sqrt{3}}, \quad (6)$$

where n_s is the number of strange quarks and $\langle L \cdot S \rangle$ is the expectation value of the spin-orbit operator acting on the whole system. Similarly the diagonal matrix elements of B_3 take the simple analytic form

$$B_3 = -n_s \frac{S(S+1)}{6\sqrt{3}}, \quad (7)$$

where S is the total spin. The contribution of B_3 is always negative, otherwise vanishing for nonstrange baryons. These formulas can be applied to ${}^28_j, {}^48_j, {}^210_j$ and ${}^21_{1/2}$ baryons of the $[70, \ell^+]$ multiplet. Presently the SU(3) breaking operators B_2 and B_3 are included in the analysis of the $[70, \ell^+]$ multiplet, first considered in Ref. [15].

4 Fit and discussion

We have performed a consistent analysis of the experimentally known resonances supposed to belong either to the symmetric $[56, 2^+]$ multiplet or to the mixed symmetric multiplet $[70, \ell^+]$ with $\ell = 0$ or 2, by using the same operator basis. Results of the fitted coefficients c_i and d_i are exhibited in Table 1 together with the values of χ_{dof}^2 for each multiplet.

The spin and flavor operators O_3 and O_4 are the dominant two-body operators and bring important $1/N_c$ corrections to the masses. The sum of c_3 and c_4 of $[70, \ell^+]$ is comparable to the value of c_3 in $[56, 2^+]$ where the equal contribution of O_3 and O_4 is included in c_3 . The contribution of the operator O_6 containing an SO(3) tensor is important especially for $[70, \ell^+]$ multiplet. Together with the spin-orbit it may lead to the mixing of doublets and quartets to be considered in further studies when the accuracy of data will increase. The incorporation of B_2 and B_3 in the mass formula of the $[70, \ell^+]$ multiplet brings more insight into the SU(6) multiplet classification of excited baryons in the $N = 2$ band.

Table 1. List of the dominant operators and their coefficients (MeV) from the mass formula (1) obtained in numerical fit for $[56, 2^+]$ in column 2 and for $[70, \ell^+]$ in column 3. The spin-orbit operator O_2 is defined by Eq. (4) for $[56, 2^+]$ and by Eq.(5) for $[70, \ell^+]$.

Operator	$[56, 2^+]$	$[70, \ell^+]$
$O_1 = N_c \mathbf{1}$	542 ± 2	631 ± 10
O_2 spin-orbit	7 ± 10	62 ± 26
$O_3 = \frac{1}{N_c} S^i S^i$	233 ± 11	91 ± 31
$O_4 = \frac{1}{N_c} \left[T^a T^a - \frac{1}{12} N_c (N_c + 6) \right]$		112 ± 22
$O_6 = \frac{1}{N_c} L^{(2)ij} G^{ia} G^{ja}$	6 ± 19	137 ± 55
$B_1 = n_s$	205 ± 14	35 ± 33
$B_2 = \frac{1}{N_c} (L^i G^{i8} - \frac{1}{2\sqrt{3}} L^i S^i)$	97 ± 40	-38 ± 121
$B_3 = \frac{1}{N_c} (S^i G^{i8} - \frac{1}{2\sqrt{3}} S^i S^i)$	197 ± 69	46 ± 159
χ_{dof}^2	1.63	1.67

4.1 The multiplet $[56, 2^+]$

The partial contribution and the calculated total mass obtained from the fit were presented in Table VI of Ref. [15] which we do not repeat here. The experimental masses were taken from the 2014 version of the Review of Particle Properties (PDG) [16], except for $\Delta(1905)5/2^+$ where we used the mass of Ref. [17] which gives a smaller χ_{dof}^2 but does not much change the fitted values of c_i and d_i . As expected, the most important sub-leading contribution comes from the spin operator O_3 . The contributions of the angular momentum-dependent operators O_2 and O_6 are comparable, but small. Among the SU(3) breaking terms, B_1 is dominant. An important remark is that in the $[56, 2^+]$ multiplet B_2 and B_3 lift the degeneracy of Λ and Σ baryons in the octets, which is not the case for the $[70, \ell^+]$ multiplet.

4.2 The multiplet $[70, \ell^+]$

As compared to Ref. [18] where only 11 resonances have been included in the numerical fit, here we consider 16 resonances, having a status of three, two or one star. This means that we have tentatively added the resonances $\Xi(2120)?^{?*}$, $\Sigma(2070)5/2^{+*}$, $\Sigma(1940)?^{?*}$, $\Xi(1950)?^{?***}$ and $\Sigma(2080)3/2^{+**}$. The masses and the error bars considered in the fit correspond to averages over data from the particle listings, except for a few which favor specific experimental values cited in the headings of Table 2.

We have ignored the $N(1710)1/2^{+***}$ and the $\Sigma(1770)1/2^{+*}$ resonances, the theoretical argument being that their masses are too low, leading to unnatural sizes for the coefficients c_i or d_i [19]. On the experimental side one can justify the removal of the controversial $N(1710)1/2^{+***}$ resonance due to the latest GWU analysis of Arndt et al. [20] where it has not been seen. We have also ignored the

$\Delta(1750)1/2^{+*}$ resonance, because neither Arndt et al. [20] nor Anisovich et al. [21] find evidence for it.

Table 2. Partial contribution and the total mass (MeV) predicted by the $1/N_c$ expansion. The last two columns give the empirically known masses and status from the 2014 Review of Particles Properties [16] unless specified by (A) from [21], (L) from [22], (Z) from [23], (G1) from [24], (B) from [25], (AB) from [26], (G2) from [27]. .

	Part. contrib. (MeV)								Total(MeV)	Experiment(MeV)	Name, status	
	c_1O_1	c_2O_2	c_3O_3	c_4O_4	c_6O_6	d_1B_1	d_2B_2	d_3B_3				
${}^4N[70, 2^+]_{\frac{7}{2}}^{7+}$	1892	62	113	28	-22	0	0	0	2073 ± 38	2060 ± 65 (A)	$N(1990)7/2^{+**}$	
${}^4\Lambda[70, 2^+]_{\frac{7}{2}}^{7+}$							35	11	-17	2102 ± 19	2100 ± 30 (L)	$\Lambda(2020)7/2^{+**}$
${}^4\Xi[70, 2^+]_{\frac{7}{2}}^{7+}$							70	22	-34	2131 ± 8	2130 ± 8	$\Xi(2120)?^{2*}$
${}^4N[70, 2^+]_{\frac{5}{2}}^{5+}$	1892	-10	113	28	57	0	0	0	2080 ± 32	2000 ± 50	$N(2000)5/2^{+**}$	
${}^4\Lambda[70, 2^+]_{\frac{5}{2}}^{5+}$							35	-2	-17	2096 ± 10	2100 ± 10	$\Lambda(2110)5/2^{+***}$
${}^4N[70, 2^+]_{\frac{3}{2}}^{3+}$	1892	-62	113	28	0	0	0	0	1972 ± 29			
${}^4\Lambda[70, 2^+]_{\frac{3}{2}}^{3+}$					0	35	-11	-17	1979 ± 39			
${}^4N[70, 2^+]_{\frac{1}{2}}^{1+}$	1892	-93	113	28	-80	0	0	0	1861 ± 33	1870 ± 35 (A)	$N(1880)1/2^{+**}$	
${}^4\Lambda[70, 2^+]_{\frac{1}{2}}^{1+}$						35	-16	-16	1869 ± 79			
${}^2N[70, 2^+]_{\frac{5}{2}}^{5+}$	1892	21	23	28	0	0	0	0	1964 ± 29	$1860 \pm {}^{120}_{60}$ (A)	$N(1860)5/2^{+**}$	
${}^2\Sigma[70, 2^+]_{\frac{5}{2}}^{5+}$					0	35	4	-3	2000 ± 18	2051 ± 25 (G1)	$\Sigma(2070)5/2^{+**}$	
${}^2N[70, 2^+]_{\frac{3}{2}}^{3+}$	1892	-31	23	28	0	0	0	0	1912 ± 21	1905 ± 30 (A)	$N(1900)3/2^{+***}$	
${}^2\Sigma[70, 2^+]_{\frac{3}{2}}^{3+}$					0	35	-6	-3	1938 ± 10	1941 ± 18	$\Sigma(1940)?^{2*}$	
${}^2\Xi[70, 2^+]_{\frac{3}{2}}^{3+}$					0	70	-11	-7	1964 ± 7	1967 ± 7 (B)	$\Xi(1950)?^{2***}$	
${}^4N[70, 0^+]_{\frac{3}{2}}^{3+}$	1892	0	113	28	0	0	0	0	2033 ± 18	2040 ± 28 (AB)	$N(2040)3/2^{+**}$	
${}^4\Sigma[70, 0^+]_{\frac{3}{2}}^{3+}$						35	0	-16	2052 ± 21	2100 ± 69	$\Sigma(2080)3/2^{+**}$	
${}^2\Delta[70, 2^+]_{\frac{5}{2}}^{5+}$	1892	-21	23	140	0	0	0	0	2034 ± 31	1962 ± 139	$\Delta(2000)5/2^{+**}$	
${}^2\Sigma^*[70, 0^+]_{\frac{1}{2}}^{1+}$	1892	0	23	140	0	35	0	-3	2087 ± 30	1902 ± 96	$\Sigma(1880)1/2^{+**}$	
${}^2\Lambda'[70, 0^+]_{\frac{1}{2}}^{1+}$	1890	0	23	-84	0	35	0	-3	1863 ± 19	1853 ± 20 (G2)	$\Lambda(1810)1/2^{+***}$	

The partial contributions and the calculated total masses obtained from the fit are presented in Table 2. Regarding the contribution of various operators we note that the good fit for $N(1880)1/2^{+**}$ was due to contribution of the spin-orbit operator O_2 of -93 MeV and of the operator O_6 which contributed with -80 MeV. The good fit also suggests that $\Sigma(1940)?^{?*}$ and $\Xi(1950)?^{?*}$ assigned by us to the $^2[70, 2^+]3/2^+$ multiplet is reasonable, thus these resonances may have $J^P = 3/2^+$, to be experimentally confirmed in the future.

The $1/N_c$ expansion is based on the $SU(6)$ symmetry which naturally allows a classification of excited baryons into octets, decuplets and singlets. In Table 2 the experimentally known resonances are presented. In addition some predictions are made for unknown resonances. Many of the partners in a given $SU(3)$ multiplet are not known. Note that Λ and Σ are degenerate in our approach. Although the operators B_2 and B_3 have different analytic forms at arbitrary N_c [15] they become identical at $N_c = 3$ for Λ and Σ in octets, thus they cannot lift the degeneracy between these hyperons, contrary to the $[56, 2^+]$ multiplet.

The present findings can be compared to the suggestions for assignments in the $[70, \ell^+]$ multiplet made in Ref. [28] as educated guesses. The assignment of $\Sigma(1880)1/2^{+**}$ as a $[70, 0^+]1/2^+$ decuplet resonance is confirmed as well as the assignment of $\Lambda(1810)1/2^{+**}$ as a flavor singlet. We agree with Ref. [28] regarding $\Lambda(2110)5/2^{+***}$ as a partner of $N(2000)5/2^{+**}$ in a spin quartet, contrary to our previous work [15] where $\Lambda(2110)5/2^{+***}$ was a member of a spin doublet, together with $N(1860)5/2^{+**}$ and $\Sigma(2070)5/2^{+*}$. This helps to restore the correct hierarchy of masses in all octets. However we disagree with Ref. [28] that $N(1900)3/2^{+***}$ is a member of a spin quartet. We propose it as a partner of $\Sigma(1940)?^{?*}$ and $\Xi(1950)?^{?*}$ in a spin doublet.

The problem of assignment is not trivial. Within the $1/N_c$ expansion method Ref. [17] suggests that $\Sigma(2080)3/2^{+**}$ and $\Sigma(2070)5/2^{+*}$ could be members of two distinct decuplets in the $[56, 2^+]$ multiplet.

Here the important result is that the hierarchy of masses as a function of the strangeness is correct for all multiplets.

Acknowledgments

Support from the Fonds de la Recherche Scientifique - FNRS under the Grant No. 4.4501.05 is gratefully acknowledged.

References

1. G. 't Hooft, Nucl. Phys. B **72** (1974) 461.
2. E. Witten, Nucl. Phys. B **160** (1979) 57.
3. J. L. Gervais and B. Sakita, Phys. Rev. Lett. **52** (1984) 87; Phys. Rev. D **30** (1984) 1795.
4. R. Dashen and A. V. Manohar, Phys. Lett. **B315**, 425 (1993); Phys. Lett. **B315**, 438 (1993).
5. K. Bardakci, Nucl. Phys. B **243** (1984) 197.
6. E. Jenkins, Phys. Lett. **B315**, 441 (1993).
7. R. Dashen, E. Jenkins, and A. V. Manohar, Phys. Rev. **D49**, 4713 (1994).
8. R. Dashen, E. Jenkins, and A. V. Manohar, Phys. Rev. **D51**, 3697 (1995).

9. E. Jenkins and R. F. Lebed, Phys. Rev. **D52**, 282 (1995).
10. J. L. Goity, Phys. Lett. B **414**, 140 (1997).
11. C. E. Carlson, C. D. Carone, J. L. Goity and R. F. Lebed, Phys. Lett. **B438**, 327 (1998); Phys. Rev. **D59**, 114008 (1999).
12. N. Matagne and F. Stancu, Nucl. Phys. A **811** (2008) 291.
13. N. Matagne and F. Stancu, Nucl. Phys. A **826** (2009) 161.
14. N. Matagne and F. Stancu, Rev. Mod. Phys. **87** (2015) 211.
15. N. Matagne and F. Stancu, Phys. Rev. D **93** (2016) no.9, 096004.
16. K. A. Olive et al. (Particle Data Group) Chin. Phys. **C38** (2014) 090001.
17. J. L. Goity, C. L. Schat and N. N. Scoccola, Phys. Lett. B **564**, 83 (2003).
18. N. Matagne and F. Stancu, Phys. Rev. D **87** (2013) 076012.
19. D. Pirjol and C. Schat, Phys. Rev. **D67**, 096009 (2003).
20. R. A. Arndt, W. J. Briscoe, I. I. Strakovsky and R. L. Workman, Phys. Rev. C **74** (2006) 045205.
21. A. V. Anisovich, R. Beck, E. Klempt, V. A. Nikonov, A. V. Sarantsev and U. Thoma, Eur. Phys. J. A **48** (2012) 15.
22. P. J. Litchfield *et al.*, Nucl. Phys. B **30** (1971) 125.
23. H. Zhang, J. Tulpan, M. Shrestha and D. M. Manley, Phys. Rev. C **88** (2013) 3, 035205.
24. G. P. Gopal, RL-80-045, C80-07-14.1-9.
25. S. F. Biagi *et al.*, Z. Phys. C **34** (1987) 175.
26. M. Ablikim *et al.* [BES Collaboration], Phys. Rev. D **80** (2009) 052004.
27. G. P. Gopal *et al.* [Rutherford-London Collaboration], Nucl. Phys. B **119** (1977) 362.
28. V. Crede and W. Roberts, Rept. Prog. Phys. **76** (2013) 076301.



$c\bar{c}$ -pentaquarks by a quark model

Sachiko Takeuchi

Japan College of Social Work, Kiyose, Tokyo 204-8555, Japan; Research Center for Nuclear Physics (RCNP), Osaka University, Ibaraki, Osaka, 567-0047, Japan; Theoretical Research Division, Nishina Center, RIKEN, Wako, Saitama 351-0198, Japan

Recent LHCb experiments have shown us that there are two resonances in the $J/\psi p$ channel in the $\Lambda_b^0 \rightarrow J/\psi p K^-$ decay: the higher peak, $P_c(4450)$, has a mass of $4449.8 \pm 1.7 \pm 2.5$ MeV and a width of $39 \pm 5 \pm 19$ MeV, while the lower and broader peak, $P_c(4380)$, has a mass of $4380 \pm 8 \pm 29$ MeV and a width of $205 \pm 18 \pm 86$ MeV. The most favorable set of the spin parity for the lower and the higher peaks is $J^P = (\frac{3}{2}^-, \frac{5}{2}^+)$. These two peaks are considered as $uudc\bar{c}$ pentaquark states [1].

In this work, we have investigated the $I(J^P) = \frac{1}{2}(\frac{1}{2}^-, \frac{3}{2}^-, \frac{5}{2}^-)$ $uudc\bar{c}$ systems. The possible flavor spin configurations of the uud in the $uudc\bar{c}$ $(0s)^5$ pentaquarks are one of the following three: (a) color-singlet spin- $\frac{1}{2}$ baryon, namely, nucleon, (b) color-octet spin- $\frac{1}{2}$, and (c) color-octet spin- $\frac{3}{2}$ uud configurations. It is found that the color-magnetic interaction, which gives an repulsion between the nucleons [2], gives an attraction to the $uudc\bar{c}$ states with the configuration (c); the expectation value of the color-magnetic interaction in that uud configuration is lower than that of the corresponding threshold.

The calculation by the quark cluster model, by which the baryon-meson scattering states as well as bound states can be investigated, shows us that the $uudc\bar{c}$ states with the above configuration (c) with the color-octet $c\bar{c}$ pair cause structures around the $\Sigma_c^{(*)}\bar{D}^{(*)}$ thresholds: one bound state, two resonances, and one large cusp are found in the $uudc\bar{c}$ negative parity channels. We argue that these resonances and cusp may correspond to, or combine to form, the negative parity pentaquark peak observed by LHCb.

Acknowledgments

This work has been done in collaboration with Dr. Makoto Takizawa, Dr. Kiyotaka Shimizu, and Dr. Makoto Oka. This work has been discussed in [3, 4]. The author would like to thank the participants of the Bled2016 workshop for various discussions.

References

1. R. Aaij *et al.* [LHCb Collaboration], Phys. Rev. Lett. **115**, 072001 (2015).
2. M. Oka, K. Shimizu and K. Yazaki, Prog. Theor. Phys. Suppl. **137**, 1 (2000).
3. S. Takeuchi and M. Takizawa, arXiv:1608.05475 [hep-ph].
4. S. Takeuchi and M. Takizawa, arXiv:1610.00091 [hep-ph].



Soliton model analysis of $SU(3)$ symmetry breaking for baryons with a heavy quark^{*}

H. Weigel, J. P. Blanckenberg

Physics Department, Stellenbosch University, Matieland 7602, South Africa

Abstract. In these proceedings we review the construction of the collective coordinate Hamiltonian that describes the spectrum of baryons with a single heavy quark and *up*, *down* or *strange* degrees of freedom in the context of chiral soliton models.

1 Introduction

This presentation is based on Ref. [1] that describes the numerical results of this soliton model analysis in detail. The derivation of the Hamilton for the (light) flavor degrees of freedom (*up*, *down*, *strange*) and, in particular, the origin of the constraint that projects onto certain flavor $SU(3)$ representations are discussed only by the way in Ref. [1]. We therefore provide more details of the derivation here.

2 Collective rotations in flavor symmetric $SU(3)$

The approach builds up from a chiral soliton generated from light flavors and heavy meson fields that are bound to the soliton. Both acquire *strangeness* components by collectively rotating in flavor $SU(3)$. Without symmetry breaking this corresponds to approximating time dependent configurations by large zero-mode fluctuations.

2.1 Chiral soliton

The major building block for the chiral soliton is the non-linear representation of the pseudoscalar mesons in form of the chiral field U but also vector mesons ρ and ω may be included. In a first step we construct the stable static soliton (with winding number one). Subsequently we approximate time dependent solutions and introduce collective coordinates for the flavor orientation $A(t) \in SU(3)$. Generically we write this as

$$U(\mathbf{r}, t) = A(t)U_0(\mathbf{r})A^\dagger(t), \quad (1)$$

^{*} Talk delivered by H. Weigel

where $U_0(\mathbf{r})$ represents the classical (static) soliton. The time dependence is most conveniently parameterized via eight angular velocities Ω_a

$$\frac{i}{2} \sum_{a=1}^8 \Omega_a \lambda_a = A^\dagger(t) \frac{dA(t)}{dt}. \quad (2)$$

The resulting collective coordinate Lagrange function has the structure

$$L_1(\Omega_a) = -E_{cl} + \frac{1}{2} \alpha^2 \sum_{i=1}^3 \Omega_i^2 + \frac{1}{2} \beta^2 \sum_{\alpha=4}^7 \Omega_\alpha^2 - \frac{N_c}{2\sqrt{3}} \Omega_8. \quad (3)$$

The term linear in the time derivative originates from the Wess–Zumino–Witten action [3] and therefore carries an explicit factor N_c (number of colors). The coefficients α^2 and β^2 are radial integrals of the profile functions and represent moments of inertia for rotations in isospace and the strangeness subspace of flavor $SU(3)$, respectively. The form of Eq. (3) is generic. The particular numerical values for the classical energy and the moments of inertia are, of course, subject to the particular model. They are reviewed in Ref. [2].

2.2 Heavy meson bound states

In the heavy flavor limit the pseudoscalar and vector meson components become degenerate [4]. In contrast to the light sector it is hence inevitable to include both components. Since the soliton configuration itself has non-zero orbital angular momentum the most strongest coupling to the solution dwells in the P-wave channel [5] (P and Q_μ are $SU(3)$ flavor spinors):

$$\begin{aligned} P &= \frac{e^{i\omega t}}{\sqrt{4\pi}} \Phi(\mathbf{r}) \hat{\mathbf{r}} \cdot \hat{\boldsymbol{\tau}} \chi, \\ Q_0 &= \frac{e^{i\omega t}}{\sqrt{4\pi}} \Psi_0(\mathbf{r}) \chi, \\ Q_i &= \frac{e^{i\omega t}}{\sqrt{4\pi}} \left[i\Psi_1(\mathbf{r}) \hat{\mathbf{r}}_i + \frac{1}{2} \Psi_2(\mathbf{r}) \epsilon_{ijk} \hat{\mathbf{r}}_j \tau_k \right] \chi, \end{aligned} \quad (4)$$

where $\chi = \chi(\omega)$ is a three component spinor that is constant in space but should be viewed as the Fourier amplitude of the heavy meson wave-function. Since the coupling to the light mesons occurs via a soliton in the isospin subspace, only the first two components of χ are non-zero. The parameterization that emerges by left multiplication with $\hat{\mathbf{r}} \cdot \hat{\boldsymbol{\tau}}$ has different profile functions and leads to the S-wave bound states.

The field equations for heavy mesons turn into coupled linear differential equations for the profile functions in eq. (4) with the soliton generating a binding potential. This (so-called bound state) approach assumes the soliton as infinitely heavy and corresponds to (formally) assuming the large N_c limit. Normalizable solutions to these differential equations only exist for certain frequencies ω below the heavy meson mass.

To quantize the Fourier amplitudes, χ as harmonic oscillators it is necessary to properly normalize the bound state profiles. The normalization condition is that occupying the bound produces one unit of heavy charge (charm or bottom). This heavy charge arises from the Noether current associated with an infinitesimal phase transformation of the heavy field. We write the Lagrange function for the heavy meson as

$$L_H(\omega) = \int d^3r \left[\frac{\omega^2}{2} \varphi^\dagger \hat{M} \varphi + \omega \varphi^\dagger \hat{\Lambda} \varphi + \varphi^\dagger \hat{H} \varphi \right] \chi^\dagger(\omega) \chi(\omega), \quad (5)$$

where $\varphi^\dagger = (\Phi, \Psi_0, \Psi_1, \Psi_2)$ contains the bound state profiles while the soliton determines the matrices \hat{M} , $\hat{\Lambda}$ and \hat{H} are matrices that also contain differential operators. Since the phase transformation in Eq. (4) can be modeled as $\omega \rightarrow \omega + \delta\omega$, the normalization condition reads

$$\left| \int d^3r [\omega \varphi^\dagger \hat{M} \varphi + \varphi^\dagger \hat{\Lambda} \varphi + \varphi^\dagger \hat{H} \varphi] \right| \stackrel{!}{=} 1. \quad (6)$$

We require absolute values because bound states with $\omega < 0$ have opposite heavy charge and eventually describe heavy pentaquarks with a heavy anti-quark. The heavy meson fields are spinors in $SU(3)$ flavor space and thus subject to the collective flavor rotation from Eq. (1),

$$P \longrightarrow A(t)P \quad \text{and} \quad Q_\mu \longrightarrow A(t)Q_\mu, \quad (7)$$

where the right hand sides contain the bound state profile functions. It is then very instructive to compute the time derivative

$$\begin{aligned} \dot{P} &= A(t) \left[i\omega + A^\dagger(t)\dot{A}(t) \right] \frac{e^{i\omega t}}{\sqrt{4\pi}} \Phi(r) \begin{pmatrix} \hat{r} \cdot \hat{\tau} \chi \\ 0 \end{pmatrix} \\ &= iA(t) \left[\omega + \frac{1}{2\sqrt{3}}\Omega_8 + \frac{1}{2} \sum_{\alpha=1}^7 \Omega_\alpha \lambda_\alpha \right] \frac{e^{i\omega t}}{\sqrt{4\pi}} \Phi(r) \begin{pmatrix} \hat{r} \cdot \hat{\tau} \chi \\ 0 \end{pmatrix} \end{aligned}$$

because it shows that $\frac{\partial L_H(\omega)}{\partial \Omega_8} = \frac{1}{2\sqrt{3}} \frac{\partial L_H(\omega)}{\partial \omega}$. Then the normalization condition enforces

$$-\frac{\partial L}{\partial \Omega_8} = \frac{1}{2\sqrt{3}} (N_c - \text{sign}(\omega) \chi^\dagger \chi) = \frac{1}{2\sqrt{3}} (N_c - N), \quad (8)$$

where we have also identified the charge of the heavy quark. Finally, the collective rotation of the bound state yields the hyperfine coupling [6]

$$L_{\text{hf}} = \rho \chi^\dagger \left(\boldsymbol{\Omega} \cdot \frac{\boldsymbol{\tau}}{2} \right) \chi, \quad (9)$$

where ρ is an integral involving all profile functions, including those of the classical soliton. The bound state also contributes to the moments of inertia, α^2 and β^2 , but numerically that contribution is negligible since the bound state is localized at the center of the soliton.

3 Symmetry breaking and mass formula

Though it is appropriate to work with $m_u = m_d$, the deviation $m_s \gg m_u$ is substantial and requires to add terms like

$$\mathcal{L}_{sb} \sim \frac{f_\pi^2 m_\pi^2}{4} \text{Tr} \left[\begin{pmatrix} 1 & 0 & 0 \\ 0 & 1 & 0 \\ 0 & 0 & x \end{pmatrix} (U + U^\dagger - 2) \right] + \dots \quad \text{where} \quad x \hat{=} \frac{2m_s}{m_u + m_d} \gg 1. \quad (10)$$

to the effective chiral Lagrangian that describe different masses and decay constants of strange and non-strange mesons¹. These symmetry breaking terms yield an explicit A dependence of the collective coordinate Lagrange function

$$\mathcal{L}_{sb} = -\frac{x}{2} \tilde{\gamma} [1 - D_{88}(A)] \quad \text{with} \quad D_{ab} = \frac{1}{2} \text{Tr} [\lambda_a A \lambda_b A^\dagger]. \quad (11)$$

Again, $\tilde{\gamma}$ is a radial integral² over all profile functions. Collecting Eqs. (3,9) and (11) and Legendre transforming to the right $SU(3)$ generators $R_a = \frac{\partial \mathcal{L}}{\partial \Omega_a}$ yields the Hamilton operator whose eigenvalues are the baryon masses that are expressed in the mass formula

$$E = E_{cl} + \left(\frac{1}{\alpha^2} - \frac{1}{\beta^2} \right) \frac{r(r+1)}{2} + \frac{\epsilon(x)}{2\beta^2} - \frac{1}{24\beta^2} (N_c - N)^2 \\ + |\omega|N + \frac{\rho}{2\alpha^2} [j(j+1) - r(r+1)] N. \quad (12)$$

The moments of inertia are the same for the light and heavy degrees of freedom as they result from a single local Lagrangian. In Eq. (12) $\epsilon(x)$ is the eigenvalue of $O_{sb} = \sum_{a=1}^8 R_a^2 + x\beta^2 \tilde{\gamma} [1 - D_{88}(A)]$ according subject to the constraint $R_8 = (N_c - N)/2\sqrt{3}$. For odd N_c and $N = 1$ this constraint requires diquark $SU(3)$ representations. The total spin is j and $r(r+1)$ is the eigenvalue of $\sum_{i=1}^3 R_i^2$. It is zero and one for the anti-symmetric and the symmetric diquark wave-functions, respectively.

Obtaining the eigenvalues $\epsilon(x)$ of the operator O_{sb} amounts to a non-perturbative treatment of light flavor symmetry breaking. Yet, the approach can be illuminated in the language of perturbation theory as it corresponds to linearly combining states that belong to different $SU(3)$ representations, but otherwise have identical quantum numbers. Possible representations are subject to the constraint on R_8 : For the physical value $N_c = 3$ representations with the lowest eigenvalue of the quadratic Casimir operator, $\sum_{a=1}^8 R_a^2$ are the anti-triplet and the sextet with $r = 0$ and $r = 1$, respectively. That is, these are the quark model representations. With symmetry breaking added an anti-fifteen-plet and a 24 dimensional representation follow suit [7]. Increasing to the next odd value, $N_c = 5$, an anti-sextet, a mixed- and a fully symmetric fifteen-plet are allowed by the constraint. The latter has $r = 2$ and does not have a counterpart for $N_c = 3$. Hence the N_c counting effects (heavy) baryon masses via modified eigenvalues of O_{sb} .

¹ Symmetry breaking for the heavy mesons, proportional to e.g. $M_{B_s}^2 - M_B^2$, is also included.

² The notation is chosen to distinguish it from $\gamma = x\tilde{\gamma}$ in the literature [2].

4 Summary

In these short proceedings we have explained the origin of the collective coordinate Hamiltonian from treating baryons with heavy quark as a heavy meson bound to a chiral soliton. The resulting spectrum and its comparison with empirical data has been discussed at length elsewhere [1]. We stress that light baryons are simultaneously described in this approach by setting $N = 0$ in Eq. (12) and in the constraint on R_8 . In particular, we have unique moments of inertia and symmetry breaking coefficients regardless of the value for N . This is in contrast to the approach of Ref. [8] that employs different Lagrangians in the light and heavy sectors.

Acknowledgments

One of us (HW) is very grateful to the organizers for providing this worthwhile workshop. This work supported in parts by the NRF under grant 77454.

References

1. J. P. Blanckenberg, H. Weigel, *Phys. Lett.* **B750**, 230 (2015).
2. H. Weigel, *Lect. Notes Phys.* **743**, 1 (2008).
3. E. Witten, *Nucl. Phys.* **B223**, 422, 433 (1983).
4. M. Neubert, *Phys. Rept.* **245**, 259 (1994).
5. J. Schechter, A. Subbaraman, S. Vaidya, H. Weigel, *Nucl. Phys.* **A590**, 655 (1995).
6. M. Harada, A. Qamar, F. Sannino, J. Schechter, H. Weigel, *Nucl. Phys.* **A625**, 789 (1997).
7. A. Momen, J. Schechter, A. Subbaraman, *Phys. Rev.* **D49**, 5970 (1994).
8. G. S. Yang, H. C. Kim, M. V. Polyakov, M. Praszalowicz, arXiv:1607.07089 [hep-ph].



Selected Recent Results from Belle on Hadron Spectroscopy

M. Bračko

University of Maribor, Smetanova ulica 17, SI-2000 Maribor, Slovenia and Jožef Stefan Institute, Jamova cesta 39, SI-1000 Ljubljana, Slovenia

Abstract. The paper reviews selected recent spectroscopy results of measurements performed with the experimental data sample collected by the Belle detector, which has been operating between 1999 and 2010 at the KEKB asymmetric-energy e^+e^- collider in the KEK laboratory in Tsukuba, Japan. The sample of collected experimental data enables various interesting measurements, including ones in hadron spectroscopy. Due to size of the data sample and complexity of experimental procedures, measurements are still being performed and new results published even now, several years after the end of the Belle detector operation. The selection of recent results presented here corresponds to the scope of the workshop and reflects interests of its participants.

1 Introduction

The Belle detector [1] at the asymmetric-energy e^+e^- collider KEKB [2] has during its operation, between 1999 and 2010, accumulated an impressive sample of data, corresponding to about 1 ab^{-1} of integrated luminosity. The KEKB collider, often called a *B Factory*, was operating mostly around the $\Upsilon(4S)$ resonance, but also at other Υ resonances, like $\Upsilon(1S)$, $\Upsilon(2S)$, $\Upsilon(5S)$ and $\Upsilon(6S)$, as well as in the nearby continuum [3]. As a result of both successful accelerator operation and an excellent detector performance, the large amount of collected experimental data enabled many valuable measurements in the field of hadron spectroscopy, including discoveries of new charmonium(-like) and bottomonium(-like) hadronic states together with studies of their properties. This paper reports on some of the recent results, selected according to the scope of the workshop.

2 Charmonium and Charmonium-like States

The charmonium spectroscopy was a well established field around the year 2000, when the two B Factories started their operation [4]. At that time the experimental spectrum of $c\bar{c}$ states below the $D\bar{D}$ threshold was in good agreement with the theoretical prediction (see e.g. ref. [5]), and with the last remaining $c\bar{c}$ states below the open-charm threshold soon to be discovered [6]. However, instead of a peaceful era, the true renaissance in the field actually started with the discoveries of the so called “XYZ” states—new charmonium-like states outside of the conventional charmonium picture.

Table 1. Results of branching fraction measurements for the B decays containing an intermediate exotic resonance. For $Z(3900)^0$ and $Z(4020)^0$ resonances the assumed masses are close to those of their charged partners.

Resonance	Decay mode	Upper limit (90% C.L.)
$X_1(3872)$	$\eta_c \pi^+ \pi^-$	3.0×10^{-5}
	$\eta_c \omega$	6.9×10^{-5}
$X(3730)$	$\eta_c \eta$	4.6×10^{-5}
	$\eta_c \pi^0$	5.7×10^{-6}
$X(4014)$	$\eta_c \eta$	3.9×10^{-5}
	$\eta_c \pi^0$	1.2×10^{-5}
$Z(3900)^0$	$\eta_c \pi^+ \pi^-$	4.7×10^{-5}
$Z(4020)^0$		1.6×10^{-5}
$X(3915)$	$\eta_c \eta$	3.3×10^{-5}
	$\eta_c \pi^0$	1.8×10^{-5}

2.1 The X(3872)-related news

The ‘‘XYZ’’ story begins in 2003, when Belle collaboration reported on $B^+ \rightarrow K^+ J/\psi \pi^+ \pi^-$ analysis¹, where a new state decaying to $J/\psi \pi^+ \pi^-$ was discovered [7]. The new state, called X(3872), was confirmed by the CDF, DØ, BABAR collaborations [8], and later also by the LHC experiments [9]. The properties of this narrow state ($\Gamma = (3.0^{+1.9}_{-1.4} \pm 0.9)$ MeV) with a mass of (3872.2 ± 0.8) MeV, which is very close to the $D^0 \bar{D}^{*0}$ threshold [10], have been intensively studied by Belle and other experiments [11]. These studies determined the $J^{PC} = 1^{++}$ assignment, and suggested that the X(3872) state is a mixture of the conventional 2^3P_1 $c\bar{c}$ state and a loosely bound $D^0 \bar{D}^{*0}$ molecular state.

In order to fully understand the nature and internal structure of the X(3872), further studies of X(3872) production and decay modes are needed. One example of such studies is the search for X(3872) production via the $B^0 \rightarrow X(3872)K^+\pi^-$ and $B^+ \rightarrow X(3872)K_S^0\pi^+$ decay modes, where the X(3872) decays to $J/\psi \pi^+ \pi^-$, which was presented by the Belle collaboration last year [12]. The analysis was performed on a data sample containing 772×10^6 $B\bar{B}$ events, yielding the first observation of the X(3872) in the decay $B^0 \rightarrow X(3872)K^+\pi^-$, with the measured branching fraction of $\mathcal{B}(B^0 \rightarrow X(3872)(K^+\pi^-)) \times \mathcal{B}(X(3872) \rightarrow J/\psi \pi^+ \pi^-) = (7.9 \pm 1.3(\text{stat}) \pm 0.4(\text{syst})) \times 10^{-6}$. The result for the $\mathcal{B}(B^+ \rightarrow X(3872)K^0\pi^+) \times \mathcal{B}(X(3872) \rightarrow J/\psi \pi^+ \pi^-) = (10.6 \pm 3.0(\text{stat}) \pm 0.9(\text{syst})) \times 10^{-6}$ shows that $B^0 \rightarrow X(3872)K^*(892)^0$ does not dominate the $B^0 \rightarrow X(3872)(K^+\pi^-)$ decay, which is in clear contrast to charmonium behaviour in the $B \rightarrow \psi(2S)K\pi$ case.

The $D^0 \bar{D}^{*0}$ molecular hypothesis of X(3872) allows for the existence of other ‘‘X(3872)-like’’ molecular states with different quantum numbers. Some of these states could be revealed in studies of decays to final states containing the η_c meson. For example, a $D^0 \bar{D}^{*0} - \bar{D}^0 D^{*0}$ combination (denoted by $X_1(3872)$) with quantum numbers $J^{PC} = 1^{+-}$ would have a mass around 3.872 GeV/ c^2 and

¹ Throughout the document, charge-conjugated modes are included in all decays, unless explicitly stated otherwise.

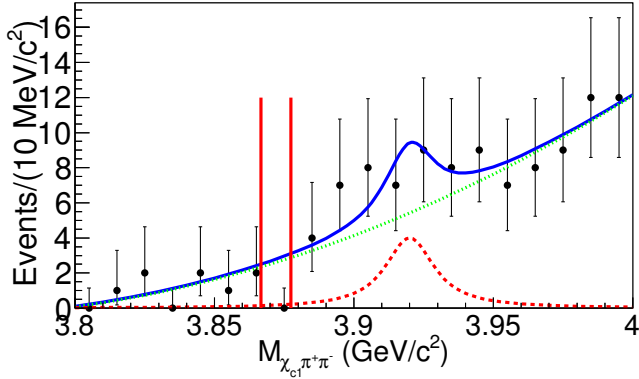


Fig. 1. The $\chi_{c1}\pi^+\pi^-$ invariant mass spectrum for $B^+ \rightarrow \chi_{c1}\pi^+\pi^-K^+$ candidates. Two vertical red lines show the $\pm 3\sigma$ window to search for $X(3872) \rightarrow \chi_{c1}\pi^+\pi^-$. The curves show the $\chi_{c1}(2P)$ signal (red dashed) and the background (green dotted) and the overall fit (blue solid).

would decay to $\eta_c\rho$ and $\eta_c\omega$. Combinations of $D^0\bar{D}^0 + \bar{D}^0D^0$, denoted by $X(3730)$, and $D^{*0}\bar{D}^{*0} + \bar{D}^{*0}D^{*0}$, denoted by $X(4014)$, with quantum numbers $J^{PC} = 0^{++}$ would decay to $\eta_c\eta$ and $\eta_c\pi^0$. The mass of the $X(3730)$ state would be around $2m_{D^0} = 3.730 \text{ GeV}/c^2$, while that of the $X(4014)$ state would be near $2m_{D^{*0}} = 4.014 \text{ GeV}/c^2$. These molecular-state candidates were searched for in the recent Belle analysis, performed on the complete Belle data sample [13]. In addition, neutral partners of the $Z(3900)^\pm$ [14] and $Z(4020)^\pm$ [15], and a poorly understood state $X(3915)$ were also searched for. All performed studies of B decays to selected final states with the η_c meson resulted in no signal being observed, thus only 90% confidence level upper limits were set on the product of branching fractions to various intermediate states and their decay branching fractions in the range $(0.6 - 6.9) \times 10^{-5}$ (see Table 1). The obtained upper limits for these exotic states are already based on the full Belle data sample and are roughly of the same order as obtained for their presumed partners (compare results from ref. [11]), so more information about the nature of these states could only be extracted from the larger data sample, which will be available at the Belle II experiment [16].

Recently Belle collaboration has studied the multi-body B decay modes with χ_{c1} and χ_{c2} in the final state, using the full Belle data sample of $772 \times 10^6 \text{ B}\bar{B}$ events [17]. This study is important to understand the detailed dynamics of B meson decays, but at the same time these decays could be exploited to search for charmonium and charmonium-like exotic states in one of the intermediate final states such as $\chi_{cJ}\pi$ and $\chi_{cJ}\pi\pi$. For example, looking at the $\chi_{c1}\pi^+\pi^-$ invariant mass spectrum in $B \rightarrow \chi_{c1}\pi^+\pi^-K$ decays, one can search for $X(3872)$ and/or $\chi_{c1}(2P)$, which could be the conventional charmonium component of the $X(3872)$ state. The $\chi_{c1}(2P)$ component may have a substantial decay rate to $\chi_{c1}\pi^+\pi^-$ because of no obvious conflict in quantum numbers and observations of di-pion transitions between χ_{bJ} states in the bottomonium system. In case

that $X(3872)$ is not a mixed state and hence $\chi_{c1}(2P)$ is a physically observable state, its decay to $\chi_{c1}\pi^+\pi^-$ would still be expected. Its mass is predicted to be about $3920 \text{ MeV}/c^2$, assuming that it lies between $\chi_{c2}(2P)$ and the $X(3915)$ that is interpreted as $\chi_{c0}(2P)$ by PDG [10]. The measurement yields $\mathcal{B}(B \rightarrow \chi_{c1}X) = (3.03 \pm 0.05(\text{stat}) \pm 0.24(\text{syst})) \times 10^{-3}$ and $\mathcal{B}(B \rightarrow \chi_{c2}X) = (0.70 \pm 0.06(\text{stat}) \pm 0.10(\text{syst})) \times 10^{-3}$. For the first time, χ_{c2} production in exclusive B decays in the modes $B^0 \rightarrow \chi_{c2}\pi^-K^+$ and $B^+ \rightarrow \chi_{c2}\pi^+\pi^-K^+$ has been observed, along with first evidence for the $B^+ \rightarrow \chi_{c2}\pi^+K_S^0$ decay mode. For χ_{c1} production, the first observation in the $B^+ \rightarrow \chi_{c1}\pi^+\pi^-K^+$, $B^0 \rightarrow \chi_{c1}\pi^+\pi^-K_S^0$ and $B^0 \rightarrow \chi_{c1}\pi^0\pi^-K^+$ decay modes is reported. For the above decay modes, a difference in the production mechanism of χ_{c2} in comparison to χ_{c1} in B decays is clearly observed. In the search for $X(3872) \rightarrow \chi_{c1}\pi^+\pi^-$ and $\chi_{c1}(2P)$, an U.L. on the product of branching fractions $\mathcal{B}(B^+ \rightarrow X(3872)K^+) \times (X(3872) \rightarrow \chi_{c1}\pi^+\pi^-) [\mathcal{B}(B^+ \rightarrow \chi_{c1}(2P)K^+) \times (\chi_{c1}(2P) \rightarrow \chi_{c1}\pi^+\pi^-)] < 1.5 \times 10^{-6} [1.1 \times 10^{-5}]$ is determined at the 90% C.L. (the fit to the $\chi_{c1}\pi^+\pi^-$ invariant mass distribution is shown in Figure 1) The negative result for these searches is compatible with the interpretation of $X(3872)$ as an admixture state of a $D^0\bar{D}^{*0}$ molecule and a $\chi_{c1}(2P)$ charmonium state.

2.2 Study of $J^{PC} = 1^{--}$ states using ISR

Initial-state radiation (ISR) has proven to be a powerful tool to search for $J^{PC} = 1^{--}$ states at B-factories, since it allows one to scan a broad energy range of \sqrt{s} below the initial e^+e^- centre-of-mass (CM) energy, while the high luminosity compensates for the suppression due to the hard-photon emission. Three charmonium-like 1^{--} states were discovered at B factories via initial-state radiation in the last decade: the $Y(4260)$ in $e^+e^- \rightarrow J/\psi\pi^+\pi^-$ [18,19], and the $Y(4360)$ and $Y(4660)$ in $e^+e^- \rightarrow \psi(2S)\pi^+\pi^-$ [20,21]. Together with the conventional charmonium states $\psi(4040)$, $\psi(4160)$, and $\psi(4415)$, there are altogether six vector states; only five of these states are predicted in the mass region above the DD threshold by the potential models [22]. It is thus very likely, that some of these states are not charmonia, but have exotic nature—they could be multiquark states, meson molecules, quark-gluon hybrids, or some other structures. In order to understand the structure and behaviour of these states, it is therefore necessary to study them in many decay channels and with largest possible data samples available.

Recent paper from Belle collaboration reports on the experimental study of the process $e^+e^- \rightarrow \gamma\chi_{cJ}$ ($J=1, 2$) via initial-state radiation using the data sample of 980 fb^{-1} , collected at and around the $\Upsilon(nS)$ ($n=1, 2, 3, 4, 5$) resonances. For the CM energy between 3.80 and 5.56 GeV, no significant $e^+e^- \rightarrow \gamma\chi_{c1}$ and $\gamma\chi_{c2}$ signals were observed except from $\psi(2S)$ decays, therefore only upper limits on the cross sections were determined at the 90% credibility level. Reported upper limits in this CM-energy interval range from few pb to a few tens of pb. Upper limits on the decay rate of the vector charmonium [$\psi(4040)$, $\psi(4160)$, and $\psi(4415)$] and charmonium-like [$Y(4260)$, $Y(4360)$, and $Y(4660)$] states to $\gamma\chi_{cJ}$ were also reported in this study (see Table 2). The obtained results could help in better understanding the nature and properties of studied vector states.

Table 2. Upper limits on $\Gamma_{ee} \times \mathcal{B}(R \rightarrow \gamma\chi_{cJ})$ at the 90% C.L.

	χ_{c1} (eV)	χ_{c2} (eV)
$\Gamma_{ee}[\psi(4040)] \times \mathcal{B}[\psi(4040) \rightarrow \gamma\chi_{cJ}]$	2.9	4.6
$\Gamma_{ee}[\psi(4160)] \times \mathcal{B}[\psi(4160) \rightarrow \gamma\chi_{cJ}]$	2.2	6.1
$\Gamma_{ee}[\psi(4415)] \times \mathcal{B}[\psi(4415) \rightarrow \gamma\chi_{cJ}]$	0.47	2.3
$\Gamma_{ee}[Y(4260)] \times \mathcal{B}[Y(4260) \rightarrow \gamma\chi_{cJ}]$	1.4	4.0
$\Gamma_{ee}[Y(4360)] \times \mathcal{B}[Y(4360) \rightarrow \gamma\chi_{cJ}]$	0.57	1.9
$\Gamma_{ee}[Y(4660)] \times \mathcal{B}[Y(4660) \rightarrow \gamma\chi_{cJ}]$	0.45	2.1

3 Results on Charmed Baryons

Recently, a lot of effort in Belle has been put into studies of charmed baryons. Many of these analyses are still ongoing, but some of the results are already available. One example of such a result is the first observation of the decay $\Lambda_c^+ \rightarrow pK^+\pi^-$ using a 980 fb^{-1} data sample [23]. This is the first doubly Cabibbo-suppressed (DCS) decay of a charmed baryon to be observed, with statistical significance of 9.4σ (fit results for invariant-mass distributions are shown in Figure 2). The branching fraction of this decay with respect to its Cabibbo-favoured (CF) counterpart is measured to be $\mathcal{B}(\Lambda_c^+ \rightarrow pK^+\pi^-)/\mathcal{B}(\Lambda_c^+ \rightarrow pK^-\pi^+) = (2.35 \pm 0.27 \pm 0.21) \times 10^{-3}$, where the uncertainties are statistical and systematic, respectively.

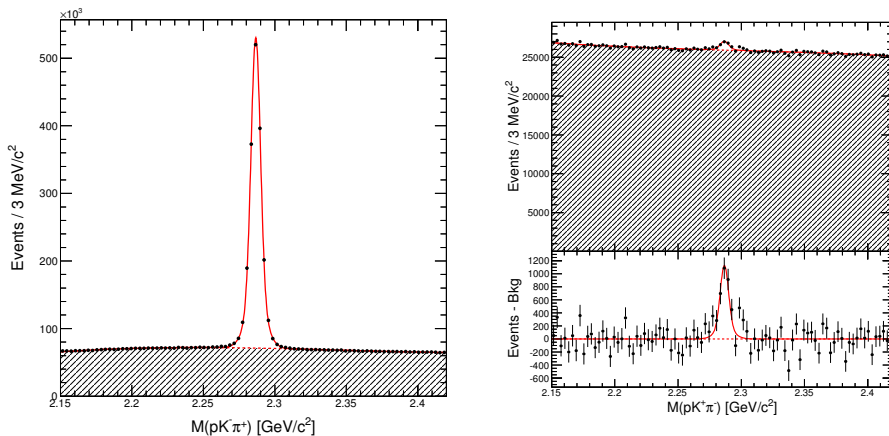


Fig. 2. Invariant mass distributions for the Λ_c^+ candidates: $M(pK^-\pi^+)$ for the CF decay mode (left) and $M(pK^+\pi^-)$ for the DCS decay mode (right, top). In the DCS case the distribution after the combinatorial-background subtraction is also shown (right, bottom). The curves indicate the fit result: the full fit model (solid) and the combinatorial background only (dashed).

4 Summary and Conclusions

Many new particles have already been discovered during the operation of the Belle experiment at the KEKB collider, and some of them are mentioned in this report. Although the operation of the experiment finished several years ago, data analyses are still ongoing and therefore more interesting results on charmonium(-like) and bottomonium(-like) and baryon spectroscopy can still be expected from Belle in the near future. These results are eagerly awaited by the community and will be widely discussed at various occasions, in particular at workshops and conferences.

Still, the era of Belle experiment is slowly coming to an end. Further progress towards high-precision measurements—with possible experimental surprises—in the field of hadron spectroscopy are expected from the huge experimental data sample, which will be collected in the future by the Belle II experiment [16].

References

1. Belle Collaboration, *Nucl. Instrum. Methods A* **479**, 117 (2002).
2. S. Kurokawa and E. Kikutani, *Nucl. Instrum. Methods A* **499**, 1 (2003), and other papers included in this Volume.
3. J. Brodzicka *et al.*, *Prog. Theor. Exp. Phys.*, 04D001 (2012).
4. A. J. Bevan *et al.*, *Eur. Phys. J. C* **74**, 3026 (2014).
5. M. B. Voloshin, *Prog. Part. Nucl. Phys.* **61**, 455 (2008).
6. Belle Collaboration, *Phys. Rev. Lett.* **89**, 102001 (2002); Cleo Collaboration, *Phys. Rev. Lett.* **95**, 102003 (2005).
7. Belle Collaboration, *Phys. Rev. Lett.* **91**, 262001 (2003).
8. CDF Collaboration, *Phys. Rev. Lett.* **93**, 072001 (2004); DØ Collaboration, *Phys. Rev. Lett.* **93**, 162002 (2004); BABAR Collaboration, *Phys. Rev. D* **71**, 071103 (2005).
9. LHCb Collaboration, *Eur. Phys. J. C* **72**, 1972 (2012); CMS Collaboration, *J. High Energy Phys.* **04**, 154 (2013).
10. K.A. Olive *et al.* (Particle Data Group), *Chin. Phys. C* **38**, 090001 (2014).
11. Belle Collaboration, *Phys. Rev. D* **84**, 052004(R) (2011); CDF Collaboration, *Phys. Rev. Lett.* **103**, 152001 (2009); LHCb Collaboration, *Phys. Rev. Lett.* **110**, 222001 (2013).
12. Belle Collaboration, *Phys. Rev. D* **91**, 051101(R) (2015).
13. Belle Collaboration, *J. High Energy Phys.* **06**, 132 (2015).
14. Belle Collaboration, *Phys. Rev. Lett.* **110**, 252002 (2013); BESIII Collaboration, *Phys. Rev. Lett.* **110**, 252001 (2013); BESIII Collaboration, *Phys. Rev. Lett.* **112**, 022001 (2014); T. Xiao, S. Dobbs, A. Tomaradze and K. K. Seth, *Phys. Lett. B* **727**, 366 (2013).
15. BESIII Collaboration, *Phys. Rev. Lett.* **111**, 242001 (2013); *Phys. Rev. Lett.* **112**, 132001 (2014).
16. Belle II Collaboration, Belle II Technical design report, [arXiv:1011.0352 [physics.ins-det]].
17. Belle Collaboration, *Phys. Rev. D* **93**, 052016 (2016).
18. BABAR Collaboration, *Phys. Rev. Lett.* **95**, 142001 (2005); *Phys. Rev. D* **86**, 051102 (2012).
19. Belle Collaboration, *Phys. Rev. Lett.* **99**, 182004 (2007).
20. Belle Collaboration, *Phys. Rev. Lett.* **99**, 142002 (2007).
21. BABAR Collaboration, *Phys. Rev. Lett.* **98**, 212001 (2007); *Phys. Rev. D* **89**, 111103 (2014).
22. S. Godfrey and N. Isgur, *Phys. Rev. D* **32**, 189 (1985); T. Barnes, S. Godfrey and E. S. Swanson, *Phys. Rev. D* **72**, 054026 (2005); G. J. Ding, J. J. Zhu and M. L. Yan, *Phys. Rev. D* **77**, 014033 (2008).
23. Belle Collaboration, *Phys. Rev. Lett.* **117**, 011801 (2016).



Puzzles in eta photoproduction: the 1685 MeV narrow peak^{*}

B. Golli^{a,c} and S. Širca^{b,c}

^a Faculty of Education, University of Ljubljana, 1000 Ljubljana, Slovenia

^b Faculty of Mathematics and Physics, University of Ljubljana, 1000 Ljubljana, Slovenia

^c and Jožef Stefan Institute, 1000 Ljubljana, Slovenia

Abstract. We claim that a narrow peak in the cross section near 1685 MeV in the $\gamma n \rightarrow \eta n$ channel can be explained through a peculiar radial behaviour of the p-wave quark states with $j = 1/2$ and $j = 3/2$ in the low lying S11 resonances and the opening of the $K\Sigma$ threshold rather than by an exotic resonance. We explain the mechanism of its formation in the framework of a coupled channel formalism which incorporates quasi-bound quark-model states corresponding to the two low lying resonances in the S11 partial wave. A relation to the Single Quark Transition Model is pointed out.

1 Motivation

In this contribution we discuss a possible quark-model explanation for a narrow structure at $W \approx 1685$ MeV in the $\gamma n \rightarrow \eta n$ reaction observed by the GRAAL Collaboration [1] which, however, turned out to be absent in the ηp channel. Azimov *et al.* [2] were the first to discuss the possibility that the structure could belong to a partner of the Θ^+ pentaquark in the exotic antidecuplet of baryons. More conventional explanations have attributed the peak to the threshold effect of the $K\Sigma$ channel [3], interference of the nearby S_{11} , P_{11} and P_{13} resonances [4], constructive and destructive interference of the two lowest S_{11} resonances in the ηn and ηp channels, respectively, as anticipated in the framework of the Giessen model [5,6] as well as in the Bonn-Gatchina analysis [7,8]. In the framework of the constituent-quark model coupled to the pseudoscalar meson octet the (non)appearance of the peak was related to different EM multipoles (at the quark level) responsible for excitation in either of the two channels [9].

2 The coupled channel approach

In our recent paper [10] we have systematically analysed the partial waves with sizable contributions to the ηN , $K\Lambda$ and $K\Sigma$ decay channels using a SU(3) extended version of the Cloudy Bag Model (CBM) [11] which includes also the ρ and ω mesons¹. We have found that the main contribution to η photoproduction

^{*} Talk delivered by B. Golli

¹ The method has been described in detail in our previous papers [12–16] where we have analysed the scattering and electro-production amplitudes in different partial waves.

at low and intermediate energies comes from the S11 partial wave. In this contribution we therefore concentrate on the S11 partial wave in which the considered phenomenon is most clearly visible.

In our approach the main contribution to η production in the S11 partial wave stems from the resonant part of the electroproduction amplitude which can be cast in the form

$$\mathcal{M}_{\eta N \gamma N}^{\text{res}} = \sqrt{\frac{\omega_\gamma E_N^\gamma}{\omega_\pi E_N}} \frac{\xi}{\pi \mathcal{V}_{N\mathcal{R}}^\pi} \langle \Psi_{\mathcal{R}} | V_\gamma | \Psi_N \rangle T_{\eta N \pi N}, \quad (1)$$

where $T_{\eta N \pi N}$ is the T-matrix element pertinent to the $\pi N \rightarrow \eta N$ channel, V_γ describes the interaction of the photon with the electromagnetic current and ξ is the spin-isospin factor depending on the considered multipole and the spin and isospin of the outgoing hadrons. Here $|\Psi_{\mathcal{R}}\rangle = c_1(W)|N(1535)\rangle + c_2(W)|N(1650)\rangle$ with

$$\begin{aligned} |N(1535)\rangle &= \cos \vartheta |70, 28, J = \frac{1}{2}\rangle - \sin \vartheta |70, 48, J = \frac{1}{2}\rangle, \\ |N(1650)\rangle &= \sin \vartheta |70, 28, J = \frac{1}{2}\rangle + \cos \vartheta |70, 48, J = \frac{1}{2}\rangle \end{aligned}$$

and $c_i(W)$ are W -dependent coefficients determined in the coupled-channel calculation for scattering.

The strong $T_{\eta N \pi N}$ amplitude is obtained in a coupled channel calculation with ten channels involving π , ρ , ω , η and K mesons. The most important channels are shown in Fig. 1. The behaviour of the amplitudes is dominated by the $N(1535)$ and $N(1650)$ resonances as well as the ηN , $K\Lambda$ and $K\Sigma$ thresholds. In the

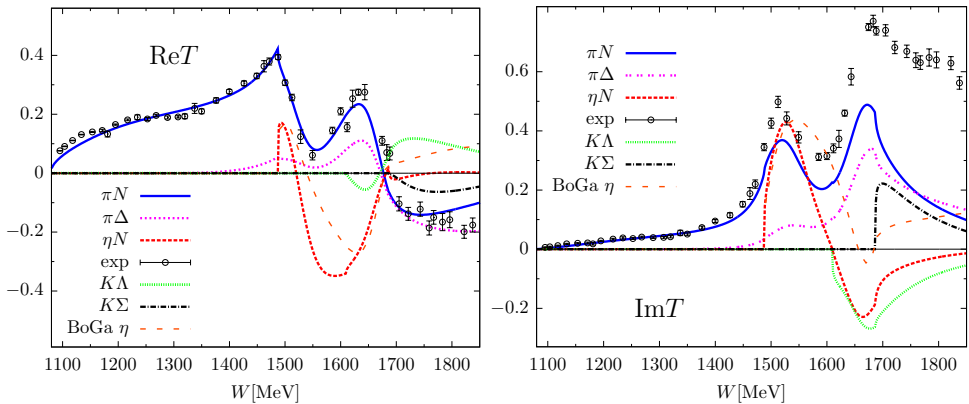


Fig. 1. The real and imaginary parts of the scattering T matrix for the dominant πN , $\pi\Delta$, ηN , $K\Lambda$ and $K\Sigma$ channels in the S11 partial wave. The corresponding thin curve denote the 2014-2 solution of the Bonn-Gatchina group [17] for the ηN channel. The data points for the elastic channel are from the SAID partial-wave analysis [18].

present calculation we put the mixing angle θ to the popular value of 30° and assume that all meson-quark coupling constants are fixed at their quark-model

values dictated by the SU(3) symmetry. While the real part of the elastic amplitude is well reproduced, the imaginary part is rather strongly underestimated in the region of the second resonance which can be to some extent attributed to too strong couplings in the $\pi\Delta$, $K\Lambda$ and $K\Sigma$ channels. This discrepancy should be taken into account when assessing the quality of the photoproduction amplitudes in the following.

3 The η photoproduction amplitudes

The electromagnetic amplitude in (1) in the S11 partial wave is dominated by the photon-quark coupling while the coupling to the pion cloud turns out to be small. The spin doublet and quadruplet states involve quarks excited to the p orbit with either $j = \frac{1}{2}$ or $j = \frac{3}{2}$ [19]:

$$|{}^4\mathbf{8}_{\frac{1}{2}}\rangle = \frac{1}{3} |(1s)^2(1p_{3/2})^1\rangle + \frac{\sqrt{8}}{3} |(1s)^2(1p_{1/2})^1\rangle, \quad (2)$$

$$|{}^2\mathbf{8}_{\frac{1}{2}}\rangle = -\frac{2}{3} |(1s)^2(1p_{3/2})^1\rangle + \frac{\sqrt{2}}{6} |(1s)^2(1p_{1/2})^1\rangle + \frac{\sqrt{2}}{2} |(1s)^2(1p_{1/2})^1\rangle', \quad (3)$$

where the last two components with $p_{1/2}$ correspond to coupling the two s-quarks to spin 1 and 0, respectively; the flavour (isospin) part is not written explicitly. The quark part of the dominant E_{0+} transition operator can be cast in the form

$$\int d\mathbf{r} \mathbf{j}^q \cdot \mathbf{A}_{11}^e = i \sum_{i=1}^3 \left[\mathcal{M}_{\frac{1}{2}} \Sigma_{11}^{[\frac{1}{2} \frac{1}{2}]}(i) + \mathcal{M}_{\frac{3}{2}} \Sigma_{11}^{[\frac{3}{2} \frac{1}{2}]}(i) \right] \left[\frac{1}{6} + \frac{1}{2} \tau_0(i) \right], \quad (4)$$

where

$$\mathcal{M}_{\frac{1}{2}} = \sqrt{\frac{2}{3}} \int d\mathbf{r} r^2 \left[j_0(qr) \left(3v_{\frac{1}{2}}^p(r) u^s(r) + u_{\frac{1}{2}}^p(r) v^s(r) \right) - 2j_2(qr) u_{\frac{1}{2}}^p(r) v^s(r) \right], \quad (5)$$

$$\mathcal{M}_{\frac{3}{2}} = \sqrt{\frac{2}{3}} \int d\mathbf{r} r^2 \left[2j_0(qr) u_{\frac{3}{2}}^p(r) v^s(r) + \frac{1}{2} j_2(qr) \left(u_{\frac{3}{2}}^p(r) v^s(r) - 3v_{\frac{3}{2}}^p(r) u^s(r) \right) \right]. \quad (6)$$

The quark transition operator is defined through $\langle l j m_j | \Sigma_{LM}^{[j \frac{1}{2}]} | \frac{1}{2} m_s \rangle = C_{\frac{1}{2} m_s LM}^{j m_j}$.

Evaluating (4) between the resonant states and the nucleon we notice that for the proton, the isoscalar part of the charge operator exactly cancels the isovector part in the case of the first two components in (2) and (3). This is a general property known as the Moorhouse selection rule [20] and follows from the fact that the flavour part in these two components corresponds to the mixed symmetric state $\phi_{M,S}$. The proton therefore receives no contribution from the $1s \rightarrow 1p_{3/2}$ transition. This is not the case with the neutron which receives contributions from all components in (2) and (3). The quark in the $1p_{3/2}$ orbit has a distinctly different radial behaviour from that in the $1p_{1/2}$ orbit, which is reflected in a different q - and W -behaviour of the amplitudes (5) and (6).

The E_{0+} amplitudes are shown in Fig. 2 for the proton and the neutron in the region of the $K\Sigma$ threshold. Our results do show a (bump-like) structure in the γn

channel, which is absent in the γp channel, though its strength in the imaginary part is lower compared to the Bonn-Gatchina 2014-2 analysis (which fits well the experimental cross-section). A moderate rise of the neutron real amplitude below the $K\Sigma$ threshold is clearly a consequence of the contribution from the $j = 3/2$ orbit, while the cusp-like drop in the amplitudes is due to the $K\Sigma$ threshold. This

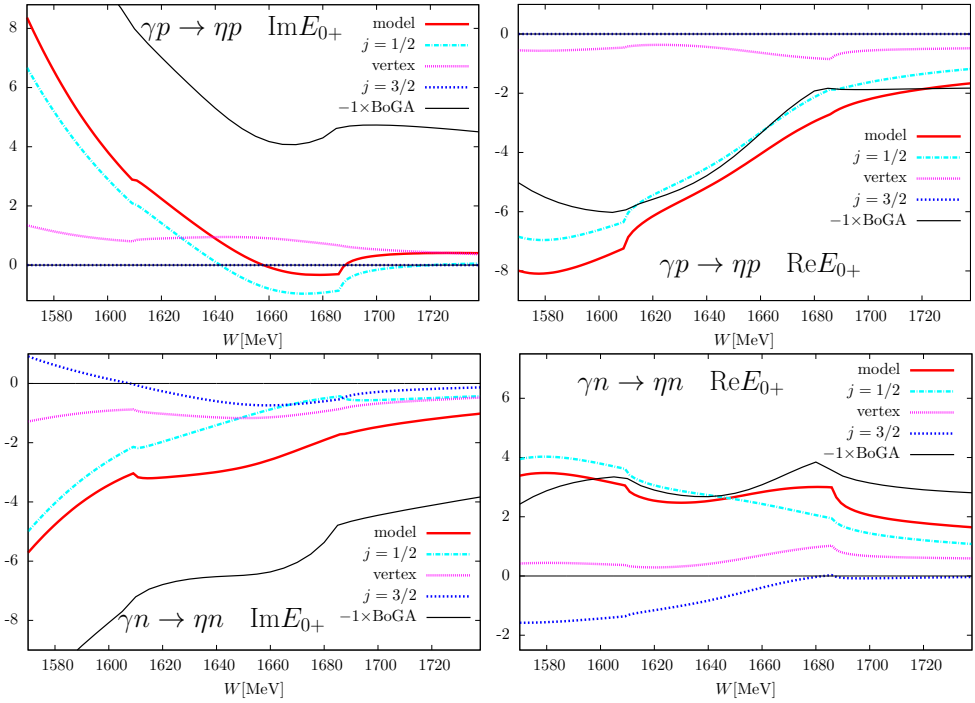


Fig. 2. The dominant contributions to the imaginary and real part of the E_{0+} amplitude (in units of mfm) for the proton (upper two panels) and for the neutron (lower two panels). Apart of the separate contributions from the $s \rightarrow p_{3/2}$ and $s \rightarrow p_{1/2}$ transitions the vertex correction is also displayed. The Bonn-Gatchina results are taken from the 2014-2 dataset and multiplied by -1 .

behaviour of the amplitudes is reflected in the cross-section as a peak (bump) present only in the neutron channel (see Fig. 3). Though the strength in our model is lower compared to the Bonn-Gatchina analysis, the qualitative agreement does offer a possible and straightforward explanation of this structure in terms of the quark model: a combination of a peculiar property of the (relativistic) wave functions of the S_{11} resonances and the presence of the $K\Sigma$ threshold. Let us stress that the proposed explanation of the considered peak would not be possible in a framework of the nonrelativistic quark model in which the radial behaviour of the quark wave function depends only on the orbital momentum quantum number.

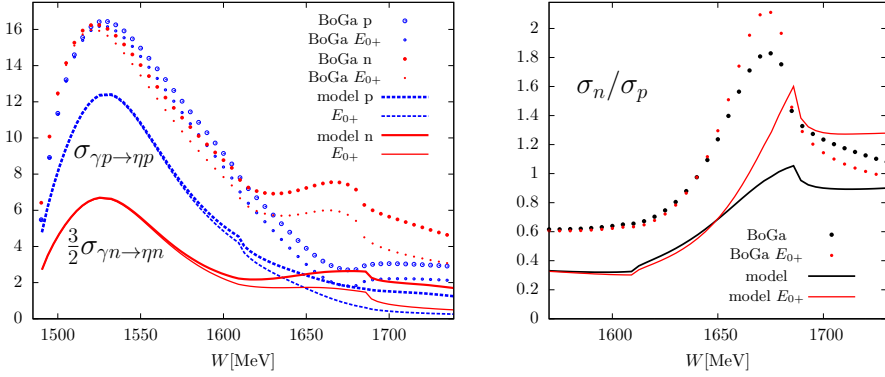


Fig. 3. The total cross-sections for $\gamma p \rightarrow \eta p$ and $\gamma n \rightarrow \eta n$ (multiplied by the conventional factor of $\frac{3}{2}$) (right panel), the ratio of the neutron and the proton cross-section (left panel). Thinner circles and lines: contribution of the S_{11} partial wave. The BoGa curves have been reconstructed from the Bonn-Gatchina 2014-2 data set [17].

4 Relation to the Single Quark Transition Model

Our model can be envisioned as a version of the Single Quark Transition Model (SQTm) in which the photon interacts with a single quark in the three-quark core and the other two quarks act as spectators. The general form of the SQTm operator is a product of the boost operator and current operators [21]:

$$B_j^\lambda = \sum_{lSL} M_{lSL}^\lambda \mathcal{T}(l, S, L, \lambda) = \sum_{l_z S} R_{l_z S}^\lambda \mathcal{T}(l, l_z, S, S_z = \lambda - l_z), \quad (7)$$

where

$$M_{lSL}^\lambda = C_{l_z S \lambda - l_z}^{L\lambda} R_{l_z S}^\lambda, \quad \langle l || T || 0 \rangle = 1 \quad \text{and} \quad \langle \frac{1}{2} || T(S) || \frac{1}{2} \rangle = \sqrt{2S+1}.$$

In our approach the quark states are labeled by the total angular momentum j , j_z rather than the orbital angular momentum and spin. In this case it is more convenient to expand (7) as

$$B_j^\lambda = \sum_{j_l L} \mathcal{M}_{j_l L}^\lambda \Sigma_{L\lambda}^{[j \frac{1}{2}]}, \quad \langle j || \Sigma_L^{[j \frac{1}{2}]} || 0 \frac{1}{2} \rangle = \delta_{j, l \pm \frac{1}{2}}.$$

Recoupling the angular momenta we find

$$\begin{aligned} \mathcal{M}_{j_l L}^\lambda &= \sum_{S=0,1} (-1)^{j+L-S-\frac{1}{2}} \sqrt{2(2L+1)(2S+1)} W(j_l S \frac{1}{2}; \frac{1}{2} L) M_{lSL}^\lambda \\ &= (-1)^{j+L-\frac{1}{2}} M_{l0l}^\lambda + (-1)^{j+L+\frac{1}{2}} \sqrt{6(2L+1)} W(j_l 1 \frac{1}{2}; \frac{1}{2} L) M_{l1L}^\lambda, \end{aligned}$$

where W are the Racah coefficients.

In the case of S_{11} resonances $l = 1$, and only the $E1$ multipole is involved ($L = 1, \lambda = 1$). In this case the coefficients (5) and (6) read

$$\begin{aligned} \mathcal{M}_{\frac{1}{2}} &= \mathcal{M}_{1 \frac{1}{2} 1} = -M_{101}^1 + \sqrt{2} M_{111}^1 = -e_1^{11} + \sqrt{2} m_1^{11}, \\ \mathcal{M}_{\frac{3}{2}} &= \mathcal{M}_{1 \frac{3}{2} 1} = M_{101}^1 + \frac{1}{\sqrt{2}} M_{111}^1 = e_1^{11} + \frac{1}{\sqrt{2}} m_1^{11}, \end{aligned}$$

where e_1^{11} and m_1^{11} are the "quark electric" and "quark magnetic" multipole moments. Table 1. in [21] gives for the corresponding E1 baryon multipole moment of the proton and the neutron which in turn can be related to (5) and (6):

$$\begin{aligned} pE1 &= \sqrt{\frac{1}{3}} e_1^{11} - \sqrt{\frac{2}{3}} m_1^{11} = -\frac{1}{\sqrt{3}} \mathcal{M}_{\frac{1}{2}}, \\ nE1 &= -\sqrt{\frac{1}{3}} e_1^{11} + \sqrt{\frac{2}{27}} m_1^{11} = \frac{1}{9\sqrt{3}} \left[5\mathcal{M}_{\frac{1}{2}} - 4\mathcal{M}_{\frac{3}{2}} \right], \end{aligned}$$

in agreement with our conclusion that the $j = \frac{3}{2}$ orbit contributes only in the $\gamma n \rightarrow \eta n$ channel, which explains the different behaviour of the ηp and ηn channels in η photoproduction.

References

1. V. Kuznetsov *et al.*, Phys. Lett. B **647**, 23 (2007).
2. Ya. Azimov *et al.* Eur. Phys. J. A **25**, 325 (2005).
3. M. Döring, K. Nakayama, Phys. Lett. B **683**, 145 (2010).
4. R. Shyam and O. Scholten, Phys. Rev. C **78**, 065201 (2008).
5. V. Shklyar, H. Lenske, U. Mosel, Phys. Lett. B **650**, 172 (2007).
6. V. Shklyar, H. Lenske, U. Mosel, Phys. Rev. C **87**, 015201 (2013).
7. A. V. Anisovich *et al.*, Eur. Phys. J. A **41**, 13 (2009).
8. A. V. Anisovich *et al.*, Eur. Phys. J. A **51**, 72 (2015).
9. X.-H. Zhong, Q. Zhao, Phys. Rev. C **84**, 045207 (2011).
10. B. Golli, S. Širca, Eur. Phys. J. A **52**, 279 (2016).
11. E. A. Veit, B. K. Jennings, A. W. Thomas, R. C. Barret, Phys. Rev. D **31**, 1033 (1985).
12. P. Alberto, L. Amoreira, M. Fiolhais, B. Golli, and S. Širca, Eur. Phys. J. A **26**, 99 (2005).
13. B. Golli and S. Širca, Eur. Phys. J. A **38**, 271 (2008).
14. B. Golli, S. Širca, and M. Fiolhais, Eur. Phys. J. A **42**, 185 (2009).
15. B. Golli, S. Širca, Eur. Phys. J. A **47**, 61 (2011).
16. B. Golli, S. Širca, Eur. Phys. J. A **49**, 111 (2013). Eur. Phys. J. A **49**, 111 (2013).
17. <http://pwa.hiskp.uni-bonn.de/>.
18. http://gwdac.phys.gwu.edu/analysis/pr_analysis.html.
19. F. Myhrer and J. Wroldsen, Z. Phys. C **25**, 281 (1984).
20. R. G. Moorhouse, Phys. Rev. Lett. **16** 772 (1996).
21. W.N. Cottingham and L.H. Dunbar, Z. Physik C **2**, 41 (1979).



The equation of state in the quasispin Nambu–Jona-Lasinio model

Mitja Rosina^{a,b}

^aFaculty of Mathematics and Physics, University of Ljubljana, Jadranska 19, P.O. Box 2964, 1001 Ljubljana, Slovenia

^bJ. Stefan Institute, 1000 Ljubljana, Slovenia

Abstract. We study to what extent the soluble two-level Nambu–Jona-Lasino model can be applied to the study of the equation of state of quark matter. We have found that in the relation of energy versus temperature the phase transition does occur at a similar temperature as in Lattice QCD calculations.

1 Introduction

We have designed a simple model similar to the Nambu–Jona-Lasino model, in order to explore pedagogically [1,2] several phenomena and approximations similar to those in full Nambu–Jona-Lasinio or Lattice QCD. In our previous studies, it was very instructive to get consistent results with such a simple model for ground state (vacuum) properties such as the chiral condensate, as well as multipion energies, pion-pion scattering length, and sigma meson energy and width [3]. In this contribution we explore the application to the phase transition of quark matter.

In order to have a soluble two-level model with finite number of quarks, we make the following simplifications:

1. We assume a sharp 3-momentum cutoff $0 \leq |\mathbf{p}_i| \leq \Lambda$;
2. The space is restricted to a box of volume \mathcal{V} with periodic boundary conditions. This gives a finite number of discrete momentum states, $\mathcal{N} = N_h N_c N_f \mathcal{V} \Lambda^3 / 6\pi^2$ occupied by N quarks. (N_h , N_c and N_f are the number of quark helicities, colours and flavours.)
3. We take an average value of kinetic energy for all momentum states: $|\mathbf{p}_i| \rightarrow P = \frac{3}{4}\Lambda$.
4. While in the NJL model the interaction conserves the sum of momenta of both quarks we assume that each quark conserves its momentum and only switches from the Dirac level to Fermi level.
5. Temporarily, we restrict to one flavour of quarks, $N_f = 1$.

We get a simplified NJL-like Hamiltonian

$$H = \sum_{k=1}^N \left(\gamma_5(k) h(k) P + m_0 \beta(k) \right) + \\ - \frac{g}{2} \left(\sum_{k=1}^N \beta(k) \sum_{l=1}^N \beta(l) + \sum_{k=1}^N i\beta(k) \gamma_5(k) \sum_{l=1}^N i\beta(l) \gamma_5(l) \right) .$$

Here γ_5 and β are Dirac matrices, $h = \boldsymbol{\sigma} \cdot \mathbf{p}/|\mathbf{p}|$, m_0 is the bare quark mass and $g = 4G/\mathcal{V}$.

We introduce the quasispin operators which obey the spin commutation relations

$$j_x = \frac{1}{2} \beta , \quad j_y = \frac{1}{2} i\beta\gamma_5 , \quad j_z = \frac{1}{2} \gamma_5 ,$$

$$R_\alpha = \sum_{k=1}^N \frac{1+h(k)}{2} j_\alpha(k) , \quad L_\alpha = \sum_{k=1}^N \frac{1-h(k)}{2} j_\alpha(k) , \quad J_\alpha = R_\alpha + L_\alpha = \sum_{k=1}^N j_\alpha(k) .$$

The model Hamiltonian can then be written as

$$H = 2P(R_z - L_z) + 2m_0 J_x - 2g(J_x^2 + J_y^2) .$$

The three model parameters $\Lambda = 648 \text{ MeV}$, $G = 40.6 \text{ MeV fm}^3$, $m_0 = 4.58 \text{ MeV}$ have been fitted (in a Hartree-Fock + RPA approximation) to the observables

$$M = \sqrt{\left(E_g(N) - E_g(N-1) \right)^2 - P^2} = 335 \text{ MeV}$$

$$Q = \langle g | \bar{\psi} \psi | g \rangle = \frac{1}{\mathcal{V}} \langle g | \sum_i \beta(i) | g \rangle = \frac{1}{\mathcal{V}} \langle g | J_x | g \rangle = 250^3 \text{ MeV}^3$$

$$m_\pi = E_1(N) - E_g(N) = 138 \text{ MeV} .$$

The values of our model parameters are very close to those of full Nambu–Jona-Lasinio model used by the Coimbra group [4] and by Buballa [5].

2 The canonical ensemble

It is easy to evaluate the matrix elements of the quasispin Hamiltonian using the angular momentum algebra. If N is not too large the corresponding sparse matrix can be diagonalized using *Mathematica*. The eigenstates and eigenvalues $\epsilon(\nu)$ are labeled with the quasispin quantum numbers R and L corresponding to the operators $|R|^2$ and $|L|^2$ which commute with the Hamiltonian. The eigenvalues may be highly degenerate (degeneracy $D(\nu)$ is due to the permutation symmetry of different single particle labels $p(i)$). The ground state band with $R = L = N/4$ is nondegenerate and corresponds to the vacuum and multipion states.

To get the equation of state (energy versus temperature) we apply the canonical ensemble

$$E = \sum \epsilon(\nu) D(\nu) \exp(-\epsilon(\nu)/T) / \sum D(\nu) \exp(-\epsilon(\nu)/T).$$

It is plotted in Fig.1 for two different values of quark numbers. As expected, the phase transition is sharper for the larger number of quarks. However, the values of energy are about the same. The model in its present form does not offer yet the thermodynamic limit in which the energy would be proportional to the volume. The reason is in the approximation $3(|\mathbf{p}_i| \rightarrow P = \frac{3}{4}\Lambda)$ which makes lifting quarks to the upper level too expensive. Only collective excitations (multipion states, σ mesons etc.) contribute significantly to the equation of state, but they are roughly independent of the size of the normalization volume. Improvements to make a more flexible average of the kinetic energy are in progress.

In the graph for the Lattice QCD *asqtad* and *p4* refer to two different improved staggered fermion actions [6]. At low temperature the curve corresponds to the meson gas with 3 light degrees of freedom while at high temperatures it corresponds free gas of quarks and gluons (18 quarks + 18 antiquarks + 16 gluons = 52 massless degrees of freedom).

Note the difference in the vertical scale in our NJL curves (energy) as compared to the Lattice QCD curve (energy density/ T^4). As mentioned before, we are not yet in the thermodynamic limit and it would not be meaningful to plot energy density. However, even in the simple model we get the temperature of the phase transition with approximately the same value and width.

3 The two-flavour case: the SU(4) algebra

In order to proceed to two flavours, a larger group than SU(2) would be needed. It is the $O(3) \otimes O(3) \subset O(5) \subset O(6)$ group (or equivalently SU(4) group) with fifteen generators

$$\tau^\alpha; \quad \gamma_5 \tau^\alpha; \quad \beta, \quad i\beta \gamma_5 \tau^\alpha; \quad \gamma_5, \quad i\beta \gamma_5, \quad \beta \tau^\alpha,$$

where τ^α are isospin operators with $\alpha = 1, 2, 3$.

With these generators we can express the two-flavour Hamiltonian

$$H = \sum_{k=1}^N \left(\gamma_5(k) h(k) P + m_0 \beta(k) \right) + \\ - \frac{g}{2} \left(\sum_{k=1}^N \beta(k) \sum_{l=1}^N \beta(l) + \sum_{k=1}^N i\beta(k) \gamma_5(k) \tau(k) \cdot \sum_{l=1}^N i\beta(l) \gamma_5(l) \tau(l) \right) .$$

Work is in progress.

We have discussed this SU(4) symmetry in 2009 but have not exploited it yet [2]. This symmetry has been recently widely popularized and applied by L.Glozman [7–11].

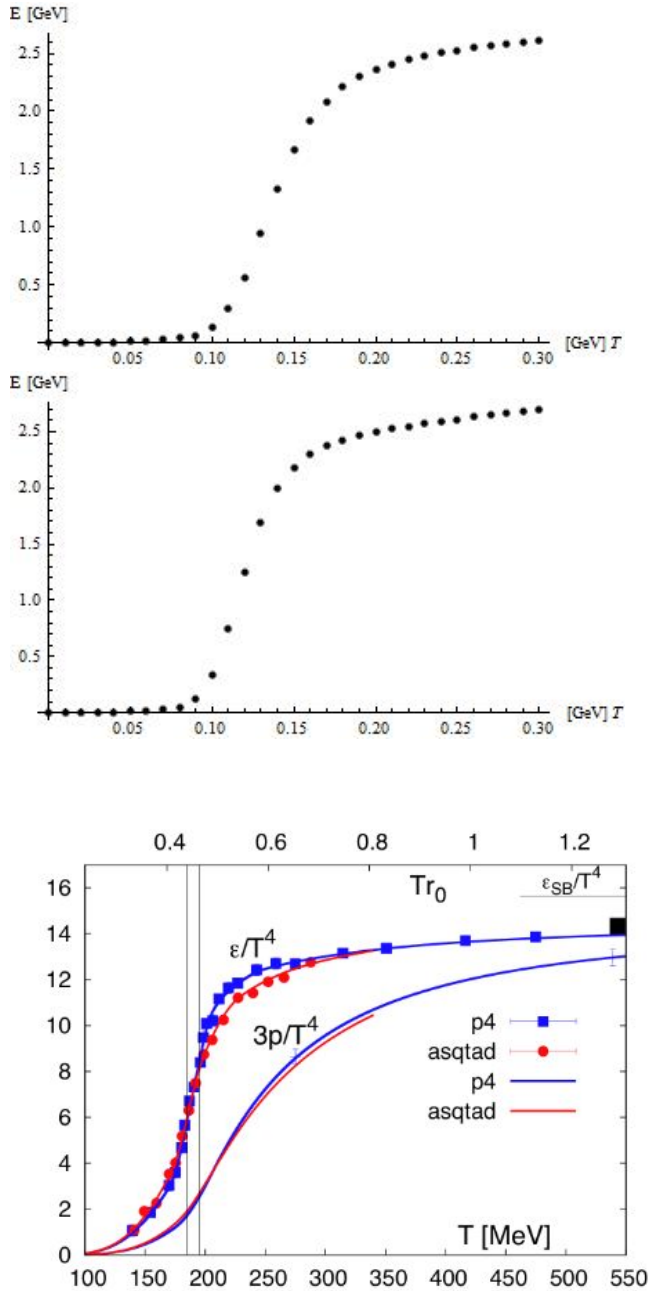


Fig. 1. Equation of state in the Quasispin NJL for $N = 96$ and $N = 192$, compared to the Lattice QCD [6]

References

1. B. T. Oblak and M. Rosina, *Bled Workshops in Physics* **7**, No. 1 (2006) 92; **8**, No. 1 (2007) 66; **9**, No. 1 (2008) 98 ; also available at <http://www-f1.ijs.si/BledPub>.
2. M. Rosina and B.T.Oblak, *Few-Body Syst.* **47** (2010) 117-123.
3. M. Rosina, *Bled Workshops in Physics* **16**, No. 1 (2015) 91.
4. M. Fiolhais, J. da Providência, M. Rosina and C. A. de Sousa, *Phys. Rev. C* **56** (1997) 3311.
5. M. Buballa, *Phys. Reports* **407** (2005) 205.
6. Bazavov et al., *Phys.Rev.D* **80**(2009)14504[arXiv:0903.4379].
7. L. Ya Glozman, arXiv:1407.2798v3 [hep-ph].
8. M. Denissenya, L. Ya Glozman, C.B. Lang, *Phys.Rev.D* **91**(2015)034505 [arXiv:1410.8751v2 [hep.lat]]; PoS(LATTICE 2014)068 [arXiv:1411.1578v1[hep-lat]].
9. L. Ya Glozman, M. Pak, arXiv:1504.02323v2 [hep-lat] .
10. M. Denissenya, L. Ya Glozman, M. Pak, *Phys.Rev.D***92**(2015) 074508 [arXiv:1508.01413[hep-ph]]; arXiv:1505.03285v1[hep-lat]; arXiv:1510.09015[hep-lat].
11. L. Ya Glozman, arXiv:1608.07269 [hep-lat].



The perennial Roper puzzle

S. Širca^{a,b}

^a Faculty of Mathematics and Physics, University of Ljubljana, Jadranska 19, 1000 Ljubljana, Slovenia

^b Jožef Stefan Institute, Jamova 39, 1000 Ljubljana, Slovenia

Abstract. A brief review of some of the recent advances regarding our knowledge of the elusive P11(1440) “Roper” resonance is presented. We refer to several experimental results from MAMI, Jefferson Lab and other laboratories; report on novel attempts at explaining the nature of this resonance within models involving meson-baryon or meson-quark dressing; and give a glimpse into the progress made in the past few years by Lattice QCD.

1 Introduction

The Roper resonance, $N^*(1440)$, which is the first excited state of the nucleon with equal quantum numbers, has been discovered in πN scattering about 50 years ago [1]. It has a very large Breit-Wigner width (extracted from partial-wave analyses), ranging from as low as 135 MeV to as high as 605 MeV according to the most recent (2016) Particle Data Group compilation of the corresponding partial-wave analyses, with an uncertainty of more than 100 MeV; its pion-nucleon scattering amplitude, $T_{\pi N}$, also has a very peculiar behavior with barely a hint of the characteristic maximum of the imaginary part at resonance. The Breit-Wigner approach at the description of the Roper is faulty by itself: the strong inelasticities simply prevent one from treating this resonance in an isolated manner.

Hence, in particular when compared to the familiar $\Delta(1232)$ excitation, the nature of the Roper remains a puzzle — in spite of it being awarded four-star PDG status. Part of the problem of course lies in the fact that it is next to impossible to observe it directly in any kind of “simple” observables like partial cross-sections. The theoretical picture is just as obscure: for example, the mechanism in Lattice QCD that would cause the positive-parity $N^*(1440)$ resonance (a radial excitation) to drift below the negative parity $N^*(1535)$ (orbital) excitation when approaching the physical pion mass, remains elusive.

2 Phenomenological support for the “two-structure” picture

Studies of the Roper resonance within dynamical coupled-channels models based on baryon-meson degrees of freedom (see, for example, [2, 3]) have shed further light into this picture by identifying multiple resonance poles originating in what

is assumed to be the same bare state. These analyses tend to yield three P_{11} poles below 2 GeV, two of which are typically associated with the $N^*(1440)$ and one with $N^*(1710)$, although it is not totally clear whether the lower-lying pair is an artefact of the analysis or a genuine statement on the resonance(s). In the most recent analysis of [3], the poles belonging to the $N^*(1440)$ are located at $(1353 - i106)$ MeV and $(1357 - i114)$ MeV, respectively.

There are several older as well as more recent experiments whose conclusions were based on the argument that indeed two structures (or mechanisms, or particular interferences involving the Roper) are needed in order to explain the observed quantities. In other words, can the two-pole structure encountered in partial-wave analysis be in any way associated with features seen in individual measurements? For example, it has been shown in the study of αp and πN scattering in the Saturne Collaboration [4,5] that the data can be explained by assuming two structures, the lower of which ($M \approx 1.39$ GeV, $\Gamma \approx 0.19$ GeV) is only seen in α -p scattering in addition to πN elastic and $\pi N \rightarrow N(\pi\pi)_S$, while the upper one ($M \approx 1.39$ GeV, $\Gamma \approx 0.19$ GeV) is seen only in πN elastic and $\pi N \rightarrow \pi\Delta$. Strong interferences of the $N^*(1440) \rightarrow N(\pi\pi)_{S-wave}^{T=0}$ and $N^*(1440) \rightarrow \pi\Delta$ processes have been claimed by [6] to be crucial in order to reproduce the $\pi\pi \rightarrow \pi\pi N$ data close to threshold as measured by the Crystal Ball collaboration. Similar conclusions were reached in the research conducted at Wasa/Promice [7] where the properties of the Roper excitation have been studied by the $pp \rightarrow pp\pi\pi$ process.

3 The Roper in quark models and on the lattice

If the Roper were a purely radial excitation (“breathing mode”) of the nucleon, corresponding to the $(1s)^3 \rightarrow (1s)^2(2s)^1$ quark transition, this should correspond to a sizeable scalar (monopole) transition strength, together with a non-zero transverse (dipole) amplitude. On the other hand, if the Roper were a $q^3 g$ hybrid, the monopole amplitude should be suppressed and the transverse part should dominate. Experimentally one observes a relatively large transverse helicity amplitude $A_{1/2}$ with a zero-crossing at $Q^2 \approx 0.5$ (GeV/c)², while the scalar helicity amplitude clearly does not vanish and is comparable in magnitude to the transverse amplitude [13], ruling out the hybrid picture. Almost all modern relativistic quark models [14–17] confirm such behavior, implying that the Roper can be seen as the first radial excitation of the q^3 ground state, although all models fail to describe the low- Q^2 behavior of $A_{1/2}$; see [19,20] for a possible remedy within a “ χ PT-inspired” effective theory and models involving strong meson-baryon dressings. Moreover, the issue of meson dressing of the quark core opens the whole avenue of exploration by means of chiral quark models (optionally incorporated into coupled-channels models). For an overview see [18].

The correct level ordering of the positive-parity $N^*(1440)$ with respect to the negative-parity $N^*(1535)$ when approaching the physical pion mass remains an unsolved problem even in the most recent lattice QCD calculations. At most, one observes “evidence” of the correct level ordering; see, for example, the studies of Refs. [21–23] and the summary plots therein, as well as the most recent calculation of Ref. [24].

4 Accessing the Roper through pion electro-production

Identifying the signatures of the Roper resonance in processes induced by real or virtual photons is an option that has been recently pursued at major electron scattering facilities like MAMI and Jefferson Lab. There is a large amount of existing data on single-pion and two-pion electroproduction processes in the energy region of the Roper resonance; see e. g. Refs. [25–30]. The most sensitive observables are single-spin and beam-target double-spin asymmetries. As such they represent crucial testing grounds for the state-of-the-art models like MAID [31] and DMT [32], two distinct approaches to meson electroproduction calculations: unitary isobar models operating with dressed resonances versus dynamical models incorporating bare states and their subsequent dynamical dressing. No such measurement has ever been performed in the region of the Roper resonance, in particular at low momentum transfers where the effects of the pion cloud are expected to be most relevant. At MAMI, we have recently performed a dedicated $p(\vec{e}, e'\vec{p})\pi^0$ experiment [10] in order to provide precise beam-recoil double polarization data for the process in the energy region of the Roper.

The differential cross section for the $p(\vec{e}, e'\vec{p})\pi$ process involving beam polarization and recoil polarization analysis can be cast in the form

$$\frac{d^5\sigma}{dp'_e d\Omega'_e d\Omega_p^*} = \Gamma \bar{\sigma} \left(1 + hA + \vec{S} \cdot \vec{\Pi} \right),$$

where Γ is the virtual photon flux, $\bar{\sigma}$ is the unpolarized cross section, h is the electron helicity, A is the beam analyzing power (equal to zero assuming parity invariance), \vec{S} is the spin direction for the recoil proton, and $\vec{\Pi} = \vec{P} + h\vec{P}'$ is the recoil polarization consisting of its helicity-independent and helicity-dependent parts. The cross section can be decomposed into products of precisely calculable kinematic factors, v_α , which depend only upon electron kinematics, with the response functions, R_α , which carry the relevant hadronic information. The central kinematics of our experiment has been chosen such that $\theta_p^* \approx 90^\circ$ and $\phi_p^* \approx 0^\circ$ (in-plane measurement), resulting in three non-vanishing polarization components:

$$\begin{aligned} P'_\ell \bar{\sigma} &= v_0 \left[v'_{LT} R'^\ell_{LT} + v'_{TT} R'^\ell_{TT} \right], \\ P_n \bar{\sigma} &= v_0 \left[v_L R^n_L + v_T R^n_T + v_{LT} R^n_{LT} + v_{TT} R^n_{TT} \right], \\ P'_t \bar{\sigma} &= v_0 \left[v'_{LT} R'^t_{LT} + v'_{TT} R'^t_{TT} \right], \end{aligned}$$

where $\bar{\sigma} = v_0 [v_L R_L + v_T R_T + v_{LT} R_{LT} + v_{TT} R_{TT}]$. The structure functions can be further represented in terms of the bilinear forms of electroproduction multipoles. For the Roper resonance the multipoles of interest are the scalar (monopole) S_{1-} and the magnetic dipole M_{1-} . To leading orders in the angular decomposition, the relevant terms in the structure functions are $R'^\ell_{TT} \propto \text{Re } E_{0+}^* (3E_{1+} + M_{1+} + 2M_{1-})$ and $R^n_T \propto \text{Im } E_{0+}^* (3E_{1+} + M_{1+} + 2M_{1-})$, hence P'_ℓ and P_n pick up the real and imaginary parts, respectively, of the same interference of the non-resonant E_{0+} multipole with the resonant M_{1-} . These interferences are the key to the sensitivity of our experiment to its Roper content as a small resonant

amplitude is multiplied by a large non-resonant one. By the same token, since $R_{LT}^{\ell} \propto \text{Re} S_{1-}^* M_{1-}$ and $R_{LT}^n \propto \text{Im} S_{1-}^* M_{1-}$, the same polarization components are also sensitive to the respective resonant-resonant interferences, but these terms are correspondingly smaller. As $P_t' \propto R_{LT}^{\ell}$, the transverse component P_t' is sensitive to two interference terms involving resonant and non-resonant amplitudes: $R_{LT}^{\ell} \propto \text{Re} [S_{\delta+}^* (2M_{1+} + M_{1-}) + (2S_{1+}^* - S_{1-}^*) E_{0+}]$.

Our study of $p(\vec{e}, e'\vec{p})\pi^0$ was performed at the three spectrometer facility of the A1 Collaboration at the Mainz Microtron (MAMI). The kinematic ranges covered were $W \approx (1440 \pm 40)$ MeV for the invariant mass, $\theta_p^* \approx (90 \pm 15)^\circ$ and $\phi_p^* \approx (0 \pm 30)^\circ$ for the CM scattering angles and $Q^2 \approx (0.1 \pm 0.02)(\text{GeV}/c)^2$ for the square of the four-momentum transfer. The analysis is ongoing.

References

1. D. Roper et al., Phys. Rev. Lett. **12** (1964) 137.
2. N. Suzuki et al., Phys. Rev. Lett. **104** (2010) 042302.
3. D. Rönchen et al., Eur. Phys. J. A **49** (2013) 44.
4. H. P. Morsch, P. Zupranski, Phys. Rev. C **61** (1999) 024002.
5. H. P. Morsch, P. Zupranski, Phys. Rev. C **71** (2005) 065203.
6. H. Kamano, M. Arima, Phys. Rev. C **73** (2006) 055203.
7. J. Pätzold et al., Phys. Rev. C **67** (2003) 052202(R).
8. K. Joo et al. (CLAS Collaboration), Phys. Rev. C **72** (2005) 058202.
9. G. V. Fedotov et al. (CLAS Collaboration), Phys. Rev. C **79** (2009) 015204.
10. H. Merkel (spokesperson), *Study of the Roper resonance in the $p(\vec{e}, e'\vec{p})\pi^0$ process*, MAMI Proposal A1-2/09.
11. J. Kelly et al. (Hall A Collaboration), Phys. Rev. Lett. **95** (2005) 102001.
12. J. Kelly et al. (Hall A Collaboration), Phys. Rev. C **75** (2007) 025201.
13. I. G. Aznauryan, V. D. Burkert, Prog. Part. Nucl. Phys. **67** (2012) 1.
14. H. J. Weber, Phys. Rev. C **41** (1990) 2783.
15. S. Kapstick, B. D. Keister, Phys. Rev. D **51** (1995) 3598.
16. F. Cardarelli et al., Phys. Lett. B **397** (1997) 13.
17. I. G. Aznauryan, Phys. Rev. C **76** (2008) 025212.
18. B. Golli, S. Širca, M. Fiolhais, Eur. Phys. J. A **42** (2009) 185.
19. T. Bauer, S. Scherer, L. Tiator, Phys. Rev. C **90** (2014) 015201.
20. S. Mokeev et al., Phys. Rev. C **86** (2012) 035203.
21. M. S. Mahbub et al., Phys. Lett. B **693** (2010) 351.
22. M. S. Mahbub et al., Phys. Lett. B **707** (2012) 389.
23. D. S. Roberts, W. Kamleh, D. B. Leinweber, Phys. Lett. B **725** (2013) 164.
24. C. B. Lang, L. Leskovec, M. Padmanath, S. Prelovsek, arXiv:1610.01422 [hep-lat].
25. V. I. Mokeev et al., Phys. Rev. C **93** (2016) 025206.
26. V. I. Mokeev et al., Phys. Rev. C **86** (2012) 035203.
27. I. G. Aznauryan et al., Phys. Rev. C **80** (2009) 055203.
28. I. G. Aznauryan et al., Phys. Rev. C **71** (2005) 015201.
29. I. G. Aznauryan et al., Phys. Rev. C **72** (2005) 045201.
30. A. S. Biselli et al., Phys. Rev. C **78** (2008) 045204.
31. D. Drechsel, S. S. Kamalov, L. Tiator, Eur. Phys. J. A **74** (2007) 69.
32. G. Y. Chen, S. S. Kamalov, S. N. Yang, D. Drechsel, L. Tiator, Phys. Rev. C **76** (2007) 035206.

Povzetki v slovenščini

Omejitve hadronskih spektrov v zvezi z lastnostmi kvarkovske snovi

Wojciech Broniowski^{a,b}

^a Institute of Physics, Jan Kochanowski University, 25-406 Kielce, Poland

^b The H. Niewodniczański Institute of Nuclear Physics, Polish Academy of Sciences, 31-342 Cracow, Poland

Opozorimo na dejstvo, da termodinamske lastnosti hadronskega plina, kot jih napoveduje kromodinamika na mreži, ne dopuščajo tako hitrega naraščanja števila resonančnih stanj v kromodinamskem spektru, kot bi ha dala Hagedornova hipoteza, razen če je med hadronskimi resonancami znaten odboj. Če bi se naraščanje po Hagedornu nadaljevalo nad 1.8 GeV, bi termodinamske funkcije znatno odstopale od vrednosti določenih na mreži pri temperaturah nad 140 MeV, ravno pod temperaturo prehoda v plazmo kvarkov in gluonov.

Kaj se lahko naučimo iz modelov tipa Nambu–Jona-Lasinio o gosti snovi?

Michael Buballa

Theoriezentrum, Institut für Kernphysik, TU Darmstadt, D-64289 Darmstadt, Germany

Podana je kritična ocena, kakšni so uspehi in omejitve modela Nambuja in Jona-Lasinia kot modela za močne interakcije pri gostoti, različni od nič. Na več primerih pokažemo, čeprav rezultatom v splošnem ne moremo zaupati kvantitativno, da je model Nambuja in Jona-Lasinia močno teoretično orodje, s katerim dobimo nove vpogleda in ideje o kromodinamskem faznem diagramu in enačbi stanja goste snovi.

Problem predznaka pri kvantni kromodinamiki

Thomas D. Cohen

Department of Physics, University of Maryland, College Park, MD 20742-4111

Mikroskopska struktura vozlišč πNN , $\pi N\Delta$ in $\pi\Delta\Delta$ v hibridnem modelu s konstituentnimi kvarki

Ju-Hyun Jung in Wolfgang Schweiger

Theoretical Physics, Institute of Physics, University of Graz, Universitaetsplatz 5, A-8010 Graz, Austria

Prikažemo mikroskopski opis močnih vozlišč πNN , $\pi N\Delta$ in $\pi\Delta\Delta$. Izhodišče je konstituentni kvarkov model z dodatkom komponente $3q\pi$. V duhu kiralnega konstituentnega kvarkovega modela smejo kvarki oddati in absorbirati pion. Ta sistem z več kanali obravnavamo relativistično invariantno v točkovni sliki. Začnemo z valovno funkcijo za N in Δ s spinsko in okusno simetrijo $SU(6)$ in izračunamo jakost omenjenih vozlišč in ustrezne oblikovne faktorje. Naši rezultati se skladajo s fenomenološko prilagojenimi količinami, dobljenimi s čisto hadronskimi večkanalskimi modeli za barionske resonance.

Spin nukleona pri globoko neelastičnem sipanju

Bogdan Povh

Max-Planck-Institut für Kernphysik, Postfach 103980, D-69029 Heidelberg, Germany

Opozorimo na konflikt pri interpretaciji deleža spina nukleona, ki ga nosijo kvarki. V kvarkovem modelu, v katerem vsebujejo oblečeni kvarki oblak mezonov π , je delež spina $\Delta\Sigma \approx 0.6$. Pri analizi globoko neelastičnega sipanja pa citirajo vrednost $\Delta\Sigma \approx 0.33$. Razpravljali smo o možnih razrešitvah tega konflikta.

Določitev deleža vrtilne količine mezona $\rho(1450)$, ki jo nosijo kiralni kvarki na mreži

C. Rohrhofer, M. Pak in L. Ya. Glozman

Theoretical Physics, Institute of Physics, University of Graz, Universitaetsplatz 5, A-8010 Graz, Austria

Delež kiralnosti in vrtilne količine za vodilno Fockovo komponento kvark-antikvark pri mezonih $\rho(770)$ in $\rho(1450)$ določimo s simulacijo na mreži s kiralnimi fermioni. Naša analiza pokaže, da je v bazi vrtilnih količin mezon $\rho(770)$ v stanju 3S_1 , v skladu s kvarkovim modelom. Stanje mezona $\rho(1450)$ pa je 3D_1 , kar kaže na napačno predpostavko v kvarkovem modelu, da je $\rho(1450)$ radialno vzbujeno stanje mezona $\rho(770)$.

Vzbujeni hiperoni iz pasu $N = 2$ v razvoju po recipročnem številu barv

Floarea Stancu

University of Liège, Institute of Physics B5, Sart Tilman, B-4000 Liège 1, Belgium

Predstavljena je ponovna analiza vzbujenih barionov z metodo razvoja po recipročnem številu barv, s posebnim poudarkom na hiperonih. Izpeljane so napovedi za klasifikacijo teh vzbujenih barionov v singlete, oktete in deкупlete grupe $SU(3)$.

Pentakvarki tipa $c\bar{c}$ v kvarkovem modelu

Sachiko Takeuchi

Japan College of Social Work, Kiyose, Tokyo 204-8555, Japan; Research Center for Nuclear Physics (RCNP), Osaka University, Ibaraki, Osaka, 567-0047, Japan; Theoretical Research Division, Nishina Center, RIKEN, Wako, Saitama 351-0198, Japan

Preučevali smo sisteme uudc \bar{c} s kvantnimi števili $I(J^P) = \frac{1}{2}(\frac{1}{2}^-, \frac{3}{2}^-, \frac{5}{2}^-)$. Možne konfiguracije uud v pentakvarku uudc \bar{c} $(0s)^5$ so barvni singlet (spin $\frac{1}{2}$), barvni oktet (spin $\frac{1}{2}$) in barvni oktet (spin $\frac{3}{2}$). Izkaže se, da kromomagnetna interakcija, ki odbija nukleone, pri tretji konfiguraciji privlači gruči uud in $c\bar{c}$ $(0s)^5$, in to pod prag za razpad. Dobimo naslednje strukture okrog pragov $\Sigma_c^{(*)}\bar{D}^{(*)}$: eno vezano stanje, dve resonanci in ost. Predvidevamo, da morda ustrezajo vrhu (pentakvarku) z negativno parnostjo, opaženem pri LHCb.

Analiza zloma simetrije $SU(3)$ pri barionih s težkim kvarkom z uporabo solitonskega modela

H. Weigel, J. P. Blanckenberg

Physics Department, Stellenbosch University, Matieland 7602, South Africa

V kontekstu kiralnega solitonskega modela podamo pregled, kako se zgradi Hamiltonov operator s kolektivnimi koordinatami, ki opiše spekter barionov z enim težkim kvarkom in lahkimi kvarki u, d in s.

Izbor novejših spektroskopskih rezultatov eksperimenta Belle

Marko Bračko

Univerza v Mariboru, Smetanova ulica 17, SI-2000 Maribor, in Institut J. Stefan, Jamova cesta 39, SI-1000 Ljubljana

Predstavljeni so nekateri novejši rezultati spektroskopskih meritev, opravljenih na vzorcu izmerjenih podatkov, ki ga je v času svojega delovanja, med letoma 1999 in 2010, zbral eksperiment Belle. Istoimenski detektor je bil postavljen ob trkalniku elektronov in pozitronov KEKB, ki je obratoval v laboratoriju KEK v Cukubi na Japonskem. Zbrani izmerjeni podatki omogočajo številne kakovostne meritve, tudi spektroskopske. Zaradi velikosti vzorca in zahtevnosti pri obdelavi izmerjenih podatkov pa raziskovalna skupina Belle objavlja rezultate novih meritev še sedaj, torej kar vrsto let po zaključku delovanja eksperimenta. Izbor rezultatov, predstavljenih v prispevku, ustreza zanimanju in razpravam udeležencev delavnice.

Uganke pri fotoprodukciji mezona eta: ozki vrh pri 1685 MeV

Bojan Golli^{a,b} in Simon Širca^{b,c}

^a Pedagoška fakulteta, Univerza v Ljubljani, Ljubljana, Slovenija

^b Institut J. Stefan, Ljubljana, Slovenija

^c Fakulteta za matematiko in fiziko, Univerza v Ljubljani, Ljubljana, Slovenija

Pokažemo, da je mogoče ozek vrh v bližini 1685 MeV v preseku za reakcijo $\gamma n \rightarrow \eta n$ razložiti z različno radialno odvisnostjo kvarkovskih stanj z $l = 1 j = 1/2$ in $l = 1 j = 3/2$ v nizko ležečih resonancah v parcialnem valu S11 in prisotnostjo praga za nastanek kaona in bariona Σ in ne kot eksotično resonanco. Razložimo mehanizem za nastanek vrha v okviru formalizma, ki vključuje kvazivezani kvarkovski stanji, ki ustrezata nizikoležečima resonancama v tem parcialnem valu. Opozorimo na povezavo z modelom SQTm, pri katerem le en sam kvark sodeluje pri vzbuditvi resonančnega stanja.

Enačba stanja v kvazispinskem modelu Nambuja in Jona-Lasinia

Mitja Rosina

Fakulteta za matematiko in fiziko, Univerza v Ljubljani, Jadranska 19, p.p.2964, 1001 Ljubljana, Slovenija in Institut J. Stefan, 1000 Ljubljana, Slovenija

Proučujemo, do katere mere se da rešljivi dvonivojski model podoben modelu Nambuja in Jona-Lasinia uporabiti tudi za študij enačbe stanja kvarkovske snovi. V povezavi energije kot funkcije temperature se res pojavi fazni prehod pri podobni temperaturi kot pri računih s kromodinamiko na mreži.

Večna uganka Roperjeve resonance

S. Širca

Fakulteta za matematiko in fiziko, Univerza v Ljubljani, Jadranska 19, p.p.2964, 1001 Ljubljana, Slovenija in Institut J. Stefan, 1000 Ljubljana, Slovenija

V prispevku podamo kratek pregled nekaterih najnovejših dognanj v zvezi z našim znanjem o skrivnostni "Roperjevi" resonanci P11(1440). Sklicujemo se na različne eksperimente iz laboratorijev MAMI, Jefferson Lab in od drugod; poročamo o novih poskusih razumevanja narave te resonance v okviru modelov z mezonsko-barionskimi in mezonsko-kvarkovskimi oblaki; in ponudimo vpogled v razvoj, ki ga je v zadnjih nekaj letih naredila kvantna kromodinamika na mreži.

BLEJSKE DELAVNICE IZ FIZIKE, LETNIK 17, ŠT. 1, ISSN 1580-4992

BLLED WORKSHOPS IN PHYSICS, VOL. 17, NO. 1

Zbornik delavnice 'Kvarki, hadroni, tvarina',
Bled, 3. – 10. julij 2016

Proceedings of the Mini-Workshop 'Quarks, Hadrons, Matter',
Bled, July 3 – 10, 2016

Uredili in oblikovali Bojan Golli, Mitja Rosina, Simon Širca

Članki so recenzirani. Recenzijo je opravil uredniški odbor.

Izid publikacije je finančno podprla Javna agencija za raziskovalno dejavnost RS iz sredstev državnega proračuna iz naslova razpisa za sofinanciranje domačih znanstvenih periodičnih publikacij.

Tehnični urednik Matjaž Zaveršnik

Založilo: DMFA – založništvo, Jadranska 19, 1000 Ljubljana, Slovenija

Natisnila tiskarna Birografika Bori v nakladi 80 izvodov

Publikacija DMFA številka 2006

Brezplačni izvod za udeležence delavnice
